TRIBHUVAN UNIVERSITY

INSTITUTE OF ENGINEERING

PULCHOWK CAMPUS

THESIS NO.: S018/075

Parametric Stability Analysis of Open Circular-Cylindrical Grid Shell

by

Thaneshwar Dhungana

A THESIS

SUBMITTED TO THE DEPARTMENT OF CIVIL ENGINEERING

IN PARTIAL FULFILLMENT OF THE REQUIREMENTS FOR THE

DEGREE OF MASTER OF SCIENCE

IN STRUCTURAL ENGINEERING

DEPARTMENT OF CIVIL ENGINEERING

LALITPUR, NEPAL

SEPTEMBER, 2021

TRIBHUVAN UNIVERSITY

INSTITUTE OF ENGINEERING

PULCHOWK CAMPUS

DEPARTMENT OF CIVIL ENGINEERING

The undersigned certify that they have read, and recommended to the Institute of Engineering for acceptance, a thesis entitled " Parametric Stability Analysis of Open Circular-Cylindrical Grid Shell" submitted by Thaneshwar Dhungana (Thesis No.: S018/075) in partial fulfilment of the requirements for the degree of Master of Science in Structural Engineering.

..……………………………………………………………

Supervisor, Dr. Hikmat Raj Joshi

Professor

Department of Civil Engineering

..……………………………………………………………

External Examiner, Dr. Govinda Prasad Lamichhane

Associate Professor

School of Engineering, Pokhara University

..……………………………………………………………

Program Co-Ordinator, Dr. Kamal Bahadur Thapa

Professor

Department of Civil Engineering

COPYRIGHT

..…………………………………

Head of Department

Department of Civil Engineering

Pulchowk Campus, Institute of Engineering

Lalitpur, Nepal

ABSTRACT

Grid shells show properties of discrete structures as well as properties of the continuous shell due to its topology. For single layered grid shells, the major failure mode is buckling. The major factors that affect the load-carrying capacity of grid shells are grid element properties, connection property, shell geometry and imperfections. Determination of buckling load of grid shell before the design process is very necessary. This is achieved by establishing equivalency between a grid shell and a continuous shell and applying the analytical equation of a continuous shell. Different equivalent models (volume, area, moment of inertia, split rigidity & orthotropic equivalency) are used to determine equivalent properties and an analytical equation for the continuous shell is modified to accommodate those properties to calculate the buckling load of the grid shell.

The geometry is an open circular-cylindrical grid shell subjected to normal load with simply supported boundary conditions. The analysis parameters are grid shape, grid size and span to depth ratio. The analytical solution is achieved by solving the buckling equation of the continuous shell for different equivalent models. A 2D Arch analysis is prepared to establish the accuracy of modelling techniques and the accuracy of FEM. A program in MATLAB is written for the analytical method. Geometries are generated in Rhino6 using the Grasshopper plugin. A numerical solution is achieved by modelling geometry and grid element properties in ANSYS and performing a linear buckling analysis. The result from the analytical and numerical methods is compared. From parametric analysis, it is concluded that a denser grid shows bending dominated characteristics whereas a coarser grid shows membrane dominated characteristics. For the denser grid, the orthotropic equivalence model for the quadrilateral grid and equivalent split rigidity for the triangular grid, and coarser grid equivalent volume model can be used to calculate the load-carrying capacity of the grid shell.

Keywords: Grid Shell, Circular-Cylindrical Shell, load-carrying capacity, equivalent model, linear buckling analysis, ANSYS

ACKNOWLEDGEMENT

I wish to express my sincere gratitude to my supervisor Prof. Dr. Hikmat Raj Joshi, for his continuous guidance, inspiration and encouragement during the thesis work and study period. His lectures and advice proved to be valuable in process of this thesis work.

I would wholeheartedly like to thank my external supervisor, Assoc. Ptof. Dr. Govinda Prasad Lamichhane for his valuable suggestions and guidance for the thesis work. Without his suggestions, this research work could not have been of this level.

I would like to thank Prof. Dr. Kamal Bahadur Thapa, our program coordinator, for providing valuable guidance throughout the progress of this thesis work. I would also like to acknowledge all the faculty members of the Department of Civil Engineering for the knowledge and concepts they gave me during my study at IOE, Pulchowk Campus.

I would like to recognize the assistance obtained through the reference books and research papers and would like to thank their authors.

Finally, I would like to appreciate the love, support and inspiration I got from my friends while doing this thesis work.

TABLE OF CONTENTS

LIST OF TABLES

LIST OF FIGURES

LIST OF SYMBOLS & ABBREVIATIONS

l	: Length of shell
L	: Span of shell
r	: Span to depth or span to rise ratio
s	: Size of grid
h	: Thickness of shell
h_{eq}	: Equivalent thickness of grid shell
a	: Radius of cylindrical shell
θ	: Angle subtended at the centre of cylindrical shell
R	: Radius of a circular arch
α	: The half-angle subtended at the centre of the circular arch
A	: Area of the element of grid shell
I	: Moment of inertia of element of grid shell
J	: Torsional moment of inertia of element of grid shell
E	: Modulus of elasticity
G	: Modulus of rigidity
ν	: Poisson's ratio
C, D	: Axial and Bending rigidity
C_{eq}, D_{eq}	: Equivalent axial and bending rigidity
ν_c, ν_D	: Poisson's ratio for axial and bending rigidity
N_x, N_θ	: Membrane normal force along X and θ direction
$N_{\theta x}, N_{x\theta}$	: Membrane shear force along X and θ direction
M_x, M_θ	: Bending moment along X and θ direction
$M_{\theta x}, M_{x\theta}$	: Twisting moment along X and θ direction
Q_x, Q_θ	: Shear force in-plane normal to along X and θ direction
u, v, w	: Displacement components along X, θ and Z direction
U_n, V_n, W_n	: Displacement components along X, θ and Z direction for n^{th} mode
n	: No. of half-wave of displacement
q	: Normal pressure load
q_c	: Buckling load

β_q	: Degree of membrane characteristics
η	: Buckling load per unit volume ratio
DR	: Dynamic relaxation
FEM	: Finite element method
MOI	: Moment of inertia

CHAPTER 1: INTRODUCTION

The objective of this thesis is to perform a parametric stability (load-carrying capacity) analysis of an open circular-cylindrical grid shell. The geometry of the grid shell under consideration is open circular-cylindrical. The span to depth ratio is varied and the load-carrying capacity of grid shells is calculated. Also, the difference in the behaviour of shells with quadrilateral and the triangular grid is analyzed.

1.1 Definition of Grid Shell

Shells exhibit more stiffness over plate structures due to their extra curvature. Continuous solid shells are more efficient in covering large spaces and carrying a load over other types of structures. Grid shells also have the properties of the continuous shell but are composed of grids rather than continuous solid-surface. In the 1960s, Frie Otto and the Institute of Lightweight Structures developed grid shells as an innovative structural system. A grid shell is described by Edmund Happold as a “doubly curved surface formed from a lattice of timber bolted together. The lattice is a mechanism with one degree of freedom" (Mesnil, 2013). More recently grid shell is defined as “a structure with the shape and strength of double curvature shell but made of a grid instead of a solid surface. The structure can cross large spans with very few materials. They can be made of any kind of material: steel, aluminium, wood and cardboard also” (Douthe, et al., 2006). Grid shells are made of one-dimensional elements. Terms like “latticed shell” or “reticulated shell” is also used for grid shell. Some of the grid shells constructed in the world are presented in Table 1.1 (Malek, 2012).

Table 1.1: Some grid shells built in the world

Year	Structures	Location
1975	Mannheim Multihalle	Mannheim, Germany
1989	Museum for Hamburg History	Hamburg, Germany
1989	Swimming Arena Neckarsulm	Neckarsulm, Germany
1994	Meeting Hall Flemish Council	Brussels, Belgium
2000	Great Court	London, United Kingdom
2000	Japan Pavilion Hanover Expo	Hanover, Germany
2002	German Historical Museum	Berlin, Germany
2011	Centre Pompidou-Metz	Metz, France
2011	National Maritime Museum	Amsterdam, Netherlands

Figure 1.1: Japan Pavilion

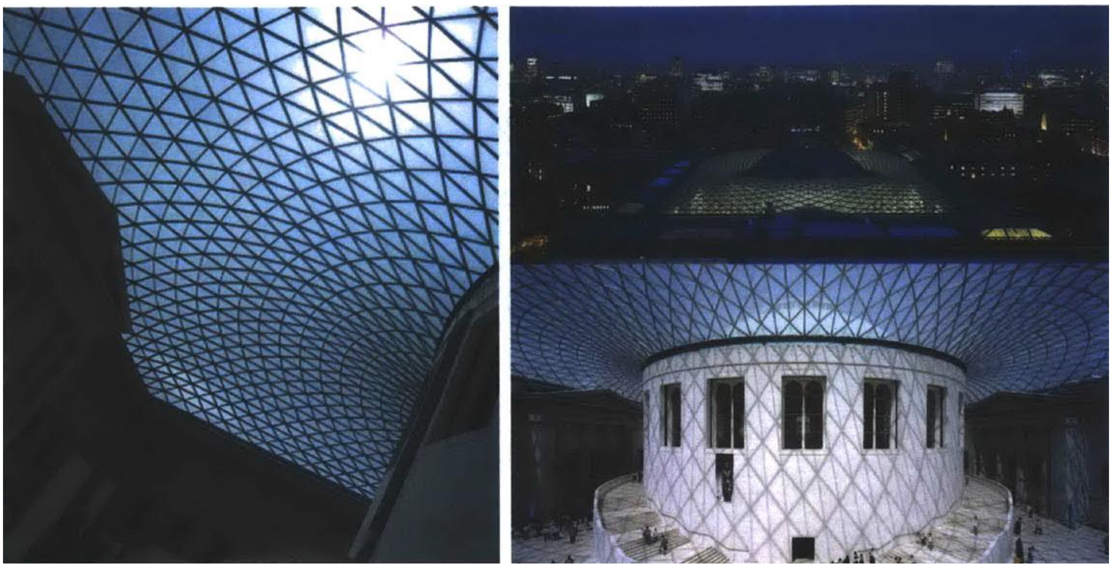

Figure 1.2: The Great Court grid shell at British Museum

1.2 Advantages of Grid Shells

Grid Shells provide great visual elegance to the structure. They are very efficient for covering large spaces. Some of the advantages of grid shells are highlighted below.

- Grid shells provide visual elegance and beauty.
- Grid shells save material to be used due to their discrete topography.
- Grid shells provide a great amount of natural lighting. The intensity of lighting can be varied by varying panel shapes and sizes.
- Grid shells are very efficient in covering existing as well as new spaces.

- Grid shells can be used as temporary structures, lightweight structures and dynamic structures as well.

1.3 Problems in Grid Shell Structure and Need of Study

Despite various advantages, grid shell has not been a structure used frequently in the world. The main reason for less use might be due to its complexity in structural analysis and construction process. There is a debate about whether a quadrilateral grid or triangular grid is efficient. Are grid shells bending or membrane dominated? How much singularity and imperfections affect the buckling load? The variation of load-carrying capacity with variation in topology and topography is also a subject of research.

1.4 Analysis Parameters

From the review of the previous works done on grid shells mentioned in Chapter 3, it can be deduced that the following are the parameters that affect the load-carrying capacity of grid shells.

- Span and depth (span to depth ratio)
- Grid shape
- Grid Size

Imperfections and Joint Rigidity are the other factors that affect the load-carrying capacity. But these factors are not in the scope of this thesis.

1.5 Objectives of the Thesis

The objectives of this thesis are: for open circular-cylindrical grid shell,

1. Compare buckling load calculated from analytical and numerical methods and suggest a better equivalent model approximation.
2. Analyze the effect of span to depth ratio, grid type (quadrilateral & triangular) and grid size on the load-carrying capacity.
3. Identify bending dominated and membrane dominated characteristics.

1.6 Assumptions and Limitations

For the progress of this thesis there are some assumptions and limitations, which are:

- The connections are considered rigid connections.
- For the dimensions selected, the grid shell is an intermediate type.
- Local instability is not considered for analysis.

- Singularity and Imperfection are not considered. The shell considered is the perfect shell.
- Shell considered is discrete and not elastically bent grid shell.

CHAPTER 2: THEORY

This chapter illustrates the necessary theoretical background for the continuum model approach and analytical solution of the buckling problem of the continuous shell. Since the aim of this thesis is to prepare a parametric stability analysis of an open circular-cylindrical grid shell, literature regarding both grid shells and buckling of shells is mentioned here.

2.1 Continuum Approach

To analyze grid shells, an approach has to be formulated. The approach considered here is the continuum approach. In this approach, some equivalencies are established between a continuous and a grid shell. A grid shell is related to a continuous shell the latter being as its calculation model. For initiation there are some basic assumptions made which are given as follows (Pshenichnov, 1993):

- The reticulated shell middle surface and those of its calculation model coincide.
- The deformation of the reticulated shell`s rod coincides with those of the calculation model.
- Force and moments in one the cross-section of the reticulated shells (after their avenging) and its calculating model are statically equivalent.

Three groups of equations define the equilibrium, strain-displacement relationship and stress-strain relationship which are: equilibrium equation, geometric equation and constitutive equations respectively. The first two groups are similar for grid shell and its continuous model. The third group differ according to grid stricture and material of grid shells.

There are various continuum approaches to define a grid shell as a continuous shell. Some of the approaches are listed below (Malek, 2012):

- Equivalent Volume: The volume of the grid shell and its equivalent continuous shell is taken as nearly equal and an equivalent thickness of the continuous shell is defined.
- Equivalent Area: The Cross-section area of the grid element of the grid shell and its equivalent continuous shell is taken as equal and an equivalent thickness of the continuous shell is defined.

- Equivalent MOI: An equivalent depth for equivalent MOI is defined for equivalent continuous shell
- Split Rigidity: Two thicknesses defined by flexural and extensional deformations are defined.
- Orthotropic: Differential equations and rigidities are derived.

2.2 Form Finding

To model and construct grid shells, the grid points are determined. Grid points collectively define the global shape (form) of the grid shells. The form of the grid shell is determined so that the forces are in equilibrium. In earlier days hanging chain models were used for form-finding. The hanging chains are in pure tension, to determine the shape in compression the model is inverted. The hanging chain model of the grid shell structure of the Herzogenriedpark building of the Mannheim Bundesgartenschau(1975) is shown in Figure 2.1 (Green & Lauri, 2017).

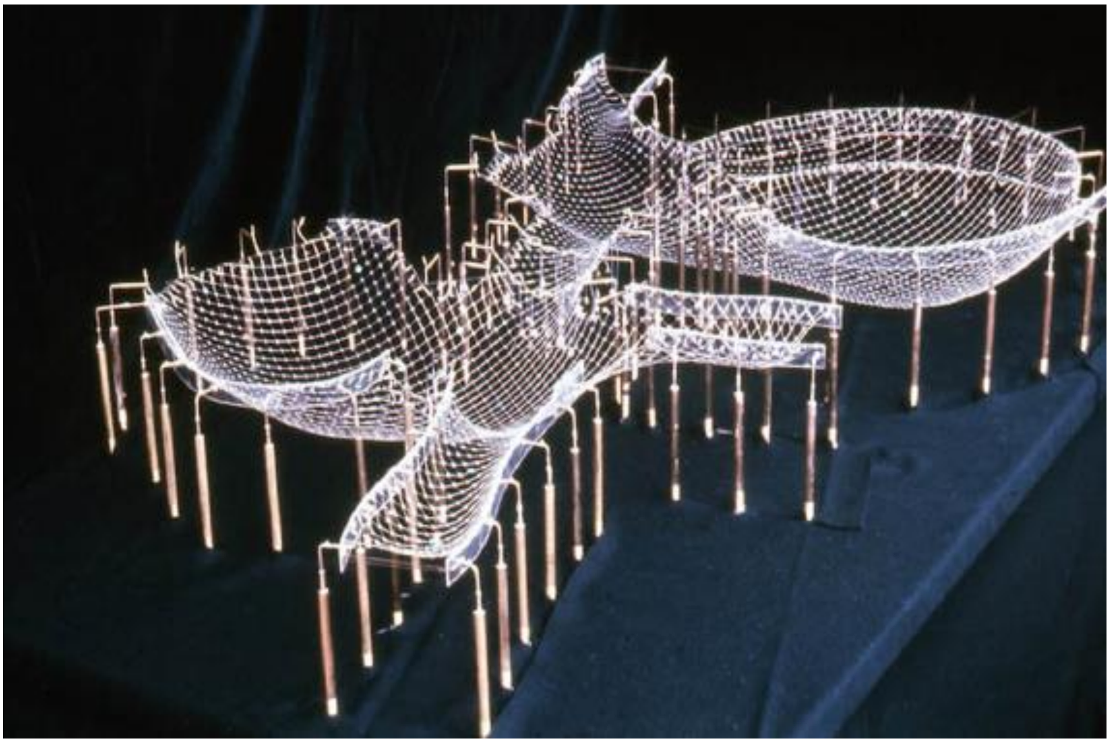

Figure 2.1: Hanging chain model of the Mannheim.

After the development of numerical tools, new methods are developed for form-finding. The Dynamic Relaxation (DR) method is used for the form-finding of grid shells. A.S. Day developed an explicit solution technique for statical analysis of structures called Dynamic Relaxation. In the DR method, the system is solved as a fictitious dynamic system within discrete time steps. Shape in equilibrium corresponding to minimum potential energy is determined.

2.3 Buckling of Shells

2.3.1 Buckling of Continuous Shells

Thin shells with certain geometric and boundary conditions carry load entirely by their membrane action. As the load is carried without bending action, we get the privilege of using small thicknesses. But with small thickness buckling action is very desirable. The load at which buckling occurs is less than the load at which failure occurs due to membrane stresses. The design of thin shells is normally dominated by the stability consideration and not merely the material strength requirement. Hence, stability analysis of thin shells acquires prime importance in designing thin shells (Farshad, 1992). Shell buckling is always disastrous, unlike a column. Bending stiffness is required to control buckling. Without bending stiffness, buckling cannot be resisted. For continuous shells, the stability and load-carrying capacity is gained from doubly curved geometry. Imperfection is very sensitive to shell buckling.

Linear and non-linear buckling analysis is done to determine the buckling load of shells. A non-linear analysis is more complicated and a closed form solution cannot be found. Linear analysis results in a fairly close value of buckling load. So, non-linear analysis is not used in the design process. The linear shell buckling analysis in the general case must be based on geometrically non-linear shell theory. The buckled shape is infinitivally close to the unbuckled shape so, the equations of the shallow shell can also be applied (Ventsel & Krauthammer, 2001).

Timoshenko and Gere (1985) has derived equilibrium equations for the circular-cylindrical shell under normal pressure loading $(X = 0, Y = 0, Z = q)$ considering non-linear shell theory. The equilibrium equations are given in Eq. 2.1.

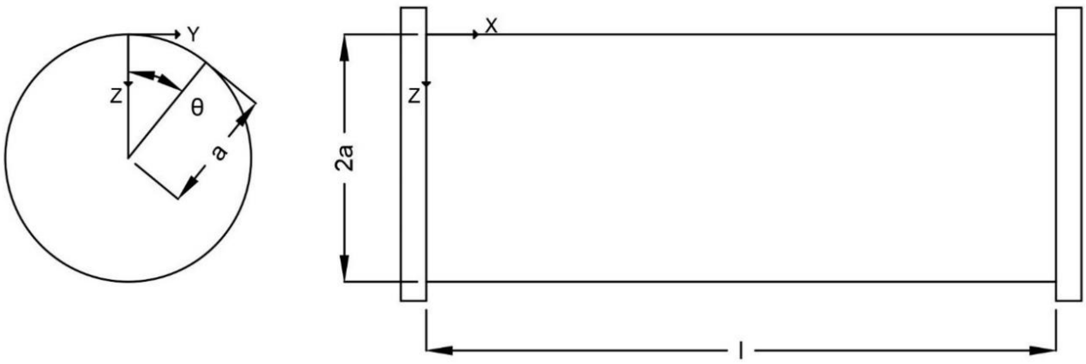

Figure 2.2: Geometrical properties and co-ordinate system of shell

$$a\frac{\partial N_x}{\partial x} + \frac{\partial N_{\theta x}}{\partial \theta} - aQ_x\frac{\partial^2 w}{\partial x^2} - aN_{x\theta}\frac{\partial^2 v}{\partial x^2} - Q_\theta\left(\frac{\partial v}{\partial x} + \frac{\partial^2 w}{\partial x \partial \theta}\right) \qquad \text{Eq. 2.1}$$

$$-N_\theta\left(\frac{\partial^2 v}{\partial x\partial\theta}-\frac{\partial w}{\partial x}\right)=0$$

$$\frac{\partial N_\theta}{\partial\theta}+a\frac{\partial N_{x\theta}}{\partial x}+aN_x\frac{\partial^2 v}{\partial x^2}-Q_x\left(\frac{\partial v}{\partial x}+\frac{\partial^2 w}{\partial x\partial\theta}\right)+N_{\theta x}\left(\frac{\partial^2 v}{\partial x\partial\theta}-\frac{\partial w}{\partial x}\right)$$

$$-Q_\theta\left(1+\frac{\partial v}{a\partial\theta}+\frac{\partial^2 w}{a\partial\theta^2}\right)=0$$

$$a\frac{\partial Q_x}{\partial x}+\frac{\partial Q_\theta}{\partial\theta}+N_{x\theta}\left(\frac{\partial v}{\partial x}+\frac{\partial^2 w}{\partial x\partial\theta}\right)+\ aN_x\frac{\partial^2 w}{\partial x^2}+N_\theta\left(1+\frac{\partial v}{a\partial\theta}+\frac{\partial^2 w}{a\partial\theta^2}\right)$$

$$+N_{\theta x}\left(\frac{\partial v}{\partial x}+\frac{\partial^2 w}{\partial x\partial\theta}\right)+qa=0$$

$$a\frac{\partial M_x}{\partial x}+\frac{\partial M_{\theta x}}{\partial\theta}+aM_{x\theta}\frac{\partial^2 v}{\partial x^2}-M_\theta\left(\frac{\partial^2 v}{\partial x\partial\theta}-\frac{\partial w}{\partial x}\right)-aQ_x=0$$

$$\frac{\partial M_\theta}{\partial\theta}+a\frac{\partial M_{x\theta}}{\partial x}+aM_x\frac{\partial^2 v}{\partial x^2}+M_{\theta x}\left(\frac{\partial^2 v}{\partial x\partial\theta}-\frac{\partial w}{\partial x}\right)-aQ_\theta=0$$

$$M_x\left(\frac{\partial v}{\partial x}+\frac{\partial^2 w}{\partial x\partial\theta}\right)-aM_{x\theta}\frac{\partial^2 w}{\partial x^2}+M_{\theta x}\left(1+\frac{\partial v}{a\partial\theta}+\frac{\partial^2 w}{a\partial\theta^2}\right)$$

$$-M_\theta\left(\frac{\partial v}{\partial x}+\frac{\partial^2 w}{\partial x\partial\theta}\right)+a(N_{x\theta}-N_{\theta x})=0$$

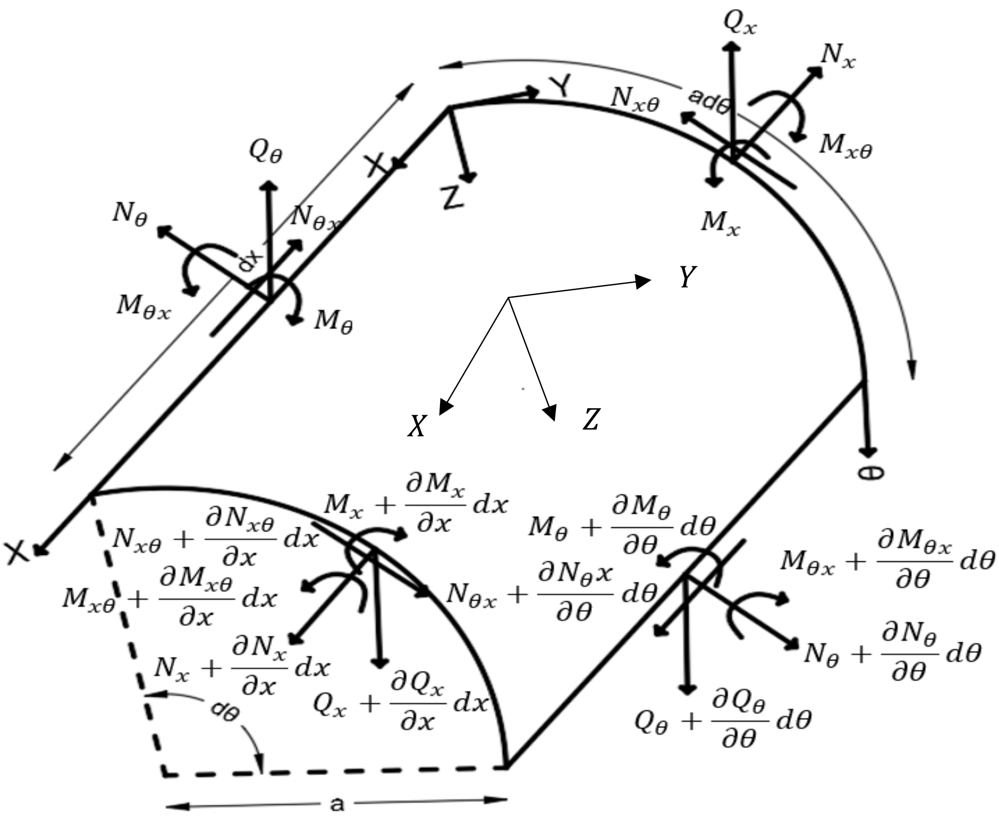

Figure 2.3: Forces and moments on the differential element of the shell

After simplification for the case of buckling under normal pressure and simply supported boundary conditions, equilibrium equations are reduced to the equations given in Eq. 2.2.

$$a\frac{\partial N_x}{\partial x}+\frac{\partial N_{\theta x}}{\partial \theta}+qa\left(\frac{\partial^2 v}{\partial x\partial \theta}-\frac{\partial w}{\partial x}\right)=0$$
$$\frac{\partial N'_\theta}{\partial \theta}+a\frac{\partial N_{x\theta}}{\partial x}-\frac{\partial M_\theta}{a\partial \theta}-\frac{\partial M_{x\theta}}{\partial x}=0 \qquad \text{Eq. 2.2}$$
$$a\frac{\partial^2 M_x}{\partial x^2}+\frac{\partial^2 M_\theta}{a\partial \theta^2}+\frac{\partial^2 M_{x\theta}}{\partial x\partial \theta}+\frac{\partial^2 M_{\theta x}}{\partial x\partial \theta}+N'_\theta-q\left(w+\frac{\partial^2 w}{\partial \theta^2}\right)=0$$

The geometric equations and constitutive equations for the circular-cylindrical shell are given in Eq. 2.3 and Eq. 2.4 respectively.

$$\epsilon_x=\frac{\partial u}{\partial x}$$
$$\epsilon_\theta=\frac{\partial v}{a\partial \theta}-\frac{w}{a}$$
$$\gamma_{x\theta}=\frac{\partial u}{a\partial \theta}+\frac{\partial v}{\partial x}$$
$$\kappa_x=-\frac{\partial^2 w}{\partial x^2} \qquad \text{Eq. 2.3}$$
$$\kappa_\theta=-\frac{1}{a^2}\left(\frac{\partial v}{\partial \theta}+\frac{\partial^2 w}{\partial \theta^2}\right)$$
$$\kappa_{x\theta}=-\frac{1}{a}\left(\frac{\partial v}{\partial x}+\frac{\partial^2 w}{\partial x\partial \theta}\right)$$

$$N_x=C(\epsilon_x+\nu_c\epsilon_\theta)$$
$$N_\theta=C(\epsilon_\theta+\nu_c\epsilon_x)$$
$$N_{x\theta}=N_{\theta x}=S=\frac{C(1-\nu_c)}{2}\gamma_{x\theta} \qquad \text{Eq. 2.4}$$
$$M_x=D(\kappa_x+\nu_D\kappa_\theta)$$
$$M_\theta=D(\kappa_\theta+\nu_D\kappa_x)$$
$$M_{x\theta}=M_{\theta x}=H=D(1-\nu_D)\kappa_{x\theta}$$

Using geometric and constitutive equations, equilibrium equations can be reduced in terms of three displacement components given in Eq. 2.5. Substituting,

$$\phi=\frac{qa}{C},\alpha=\frac{D}{Ca^2}$$

$$\left(a^2\frac{\partial^2 u}{\partial x^2}+\frac{1-\nu_c}{2}\frac{\partial^2 u}{\partial\theta^2}\right)+\frac{a(1+\nu_c)}{2}\frac{\partial^2 v}{\partial x\partial\theta}-\nu_c a\frac{\partial w}{\partial x}+\phi a\left(\frac{\partial^2 v}{\partial x\partial\theta}-\frac{\partial w}{\partial x}\right)$$
$$=0$$
$$\frac{a(1+\nu_c)}{2}\frac{\partial^2 u}{\partial x\partial\theta}+\left(\frac{a^2(1-\nu_c)}{2}\frac{\partial^2 v}{\partial x^2}+\frac{\partial^2 v}{\partial\theta^2}\right)-\frac{\partial w}{\partial\theta}$$
$$+\alpha\left(a^2(1-\nu_D)\frac{\partial^2 v}{\partial x^2}+\frac{\partial^2 v}{\partial\theta^2}+a^2\frac{\partial^3 w}{\partial x^2\partial\theta}+\frac{\partial^3 w}{\partial\theta^3}\right)=0 \qquad \text{Eq. 2.5}$$
$$a\nu_c\frac{\partial u}{\partial x}+\frac{\partial v}{\partial\theta}-\alpha\left(\frac{\partial^3 v}{\partial\theta^3}+(2-\nu_D)a^2\frac{\partial^3 v}{\partial x^2\partial\theta}+a^4\frac{\partial^4 w}{\partial x^4}+\frac{\partial^4 w}{\partial\theta^4}\right.$$
$$\left.+2a^2\frac{\partial^4 w}{\partial x^2\partial\theta^2}\right)-w-\phi\left(w+\frac{\partial^2 w}{\partial\theta^2}\right)=0$$

For simply supported boundary condition, the force and displacement component at boundaries ($x=0,l$) are $v=0, w=0, N_x=0, M_x=0$. To satisfy these boundary conditions, the displacement components are represented in double-sine series which are given in Eq. 2.6.

$$u=U_n\cos\frac{\pi x}{l}cosn\theta$$
$$v=V_n\sin\frac{\pi x}{l}sinn\theta \qquad \text{Eq. 2.6}$$
$$w=W_n\sin\frac{\pi x}{l}cosn\theta$$

Substituting displacement components in Eq. 2.5 we get,

$$\lambda=\frac{\pi x}{l}$$
$$\left(-\lambda^2-\frac{1-\nu_c}{2}n^2\right)U_n+\left(\frac{1+\nu_c}{2}n\lambda+n\lambda\phi\right)V_n+\lambda(\nu_c+\phi)W_n=0$$
$$\left(\frac{1+\nu_c}{2}n\lambda\right)U_n-\left(\frac{1-\nu_c}{2}\lambda^2+n^2+\alpha(1-\nu_D)\lambda^2+\alpha n^2\right)V_n$$
$$-(n+\alpha n\lambda^2+\alpha n^3)W_n=0 \qquad \text{Eq. 2.7}$$
$$(\nu_c\lambda)U_n-(n+\alpha n^3+\alpha(2-\nu_D)n\lambda^2)V_n$$
$$-\left(1+\alpha\lambda^4+\alpha n^4+2\alpha n^2\lambda^2+\phi(1-n^2)\right)W_n=0$$

Eq. 2.7 yields a trivial solution which is $U_n=V_n=W_n=0$. But for buckling deformation values of U_n, V_n & $W_n\neq 0$. For buckling, determinant of the Eq. 2.7 must be zero which leads to a quadric equation where only q and n are unknown. Though n is considered as continuous variable, it is actually an integer variable. The minimum value of q is critical load or buckling load and corresponding value of n is no, of half wave of deformation.

2.3.2 Buckling of Grid Shells

Grid shells carry their loads mainly by compression force. It has been well established that buckling is the dominant failure mode of single-layered grid shells (Gioncu, 1985). In a single-layer grid shell, the problem of buckling comes forward. It is assumed that individual member of the grid shell remains straight and stable during buckling. Grid shells exhibit common features of both framed structures and solid shells. Various researches have been done on the buckling of grid shells and their mechanics. Some of them has been mentioned in Chapter 3.

CHAPTER 3: LITERATURE REVIEW

Gioncu (1995) has given a detailed overview of the state-of-the-art on buckling of reticulated shells. He has mentioned fundamentally important factors in the buckling of reticulated shells which are:

- Form or Global Shape: Classification based on their Gaussian-Curvature
- Reticulation Form: Triangular and Quadrilateral Shapes
- Structural Element: Strut or Beam or Single or Double Layer
- Connections: Joint System

A grid shell has been defined as a special structural system that consists of a quadrilateral internal structure, beam element, and rigid joints. For ideal shells the loss of stability can be produced by two instability points; limit point and bifurcation point. Two main approaches: the equivalent continuum method and discrete method, to analyze buckling load for reticulated shells has been illustrated and uncertainties involved in those methods have been highlighted. Local buckling is a dangerous form of instability in reticulated shells. Various instability modes have been identified which are:

- Member Instability: When buckling of individual members occurs.
- Node Instability: When all member connected to a node undergoes axial strain.
- Torsional Instability: When bending rigidity in the surface plan is weaker.
- Line Instability: when all the nodes of a ring of a dome and the connected members are involved in the loss of stability.

Forman and Hutchinson (1970) has presented buckling analysis of few reticulated shells with both equivalent continuum analysis and discrete analysis which is regarded as exact analysis. To model a simple shell buckling problem, buckling of an axially compressed infinite reticulated beam has been formulated considering varying joint rigidity. Discrete analysis has been done applying the principle of virtual work. A shallow section of reticulated spherical shell and infinite reticulated cylindrical shell with the triangular (equilateral) grid has been analyzed using both equivalent continuum and discrete analysis. In continuum analysis equivalent flexural rigidity, axial rigidity, Poisson's ratio and load has been defined for equivalent continuous shell and its buckling load has been determined. In discrete analysis, member equations and equilibrium equations have been established and are solved as an eigenvalue problem.

Sumec (1992) has performed linear stability analysis of grid shells. It has been stated that in single layer grid shell, the problem of stability comes forward than the material strength (failure). The grid shell with a triangular grid has been analyzed with a continuum approach. The shape of a buckled segment of the surface has been assumed as a spherical segment. Applying the equivalent rigidity model and theory of finite deflection of shell, governing equations of shallow grid shell has been derived. Initial shape imperfection has also been taken into account in governing equation. Applying the Bubnov-Galerkin method, an analytical closed-form formulation for critical pressure has been derived. The rigidity of joints (rigid & hinged) has been taken into account. Some numerical examples have been presented to know the effect of radius of curvature & element length of grid shell on the critical pressure. It has been concluded that:

- The factors on which critical external normal pressure depends are the radius of curvature of grid shell, length of grid element & their sectional characteristics, material properties & initial shape imperfection of the shell and type of connecting nodes.
- For grid shells with hinged or rigid joints and an ordinary continuum model, the formula derived in closed form is an available tool.

Mesnil, et al. (2017) has done a comparative analysis of linear buckling load of grid shells with kagome grid and quadrangular grid. A strategy has been proposed for the covering of kagome meshes with planner's faces. Barrel vault and dome structures have been chosen for analysis. A method to convert quadrilateral meshes to kagome meshes has been derived. The analysis parameters chosen are aspect ratio, span to depth ratio, structural density ratio, buckling ratio and structural efficiency. A circular hollow section made of steel has been used as a grid element and support has been supposed to be pin joints. A uniform vertical projected load and non-symmetrical load has been applied as two load cases. A linearized buckling analysis has been performed for different values analysis parameters. The sensitivity of the kagome grid shell to geometrical imperfections has also been discussed. It has been concluded that the kagome grid has significantly higher performance compared to the quadrilateral grid for both symmetric and non-symmetric load cases.

Bulenda and Knippers (2001) has explained some parameters influencing the failure load of domes & barrel vaults and has made suggestions for the imperfection in shape. Non-linear finite element analysis of the imperfect structure has been performed to check the stability of the grid shell. Stability behaviour and factors affecting the stability of grid shell has been discussed. Imperfection types, method of application and scaling has been illustrated. Paraboloid over a circle and parabolic barrel vault shape has been considered for analysis. Boundary condition (hinged & rigid), the height of shell and height to span ratio have been taken as analysis parameters. A geometrically non-linear analysis has been performed and the load-displacement curve has been computed incrementally via the load control method. It has been concluded that the dome structure is very imperfection sensitive and barrel vaults are less imperfection sensitive but carry much less load.

Mesnil (2013) has studied the influence of pre-stress on the stability of elastic grid shells. A parametric study has been conducted which focuses on both pre-buckled arch and initially flat circular elastic grid shell with different grid spacing and levels of pre-stress. Realistic values for analysis parameters have been determined from existing projects. A hollow circular section has been used as a grid element. A pre-buckled 2D Arch has been chosen for the validation of the computational method. Firstly, a comparative analysis of the buckling capacity of the unstressed and pre-stressed arch has been prepared. Secondly, the buckling analysis, as well as the form-finding of different structures, have been performed using finite element analysis. The parameters that have been chosen to describe the problem are grid spacing, the height of the structure after form-finding, bending stiffness of beam and the critical line load. It has been concluded that:

- For high levels of pre-stress, an elastic grid shell and grid shell have the same bending mode shapes.
- Elastic grid shells are subject to two competing effects: the geometrical stiffens and loss of stiffness due to pre-stress.
- Elastic grid shells behave similarly to rigid grid shells. So, the tools developed for rigid grid shells could be applied to elastic grid shells.

Malek (2012) has done a parametric study of the buckling load of grid shells varying the topology and topography. A Spherical-cap and corrugated barrel vault have been chosen for analysis. For spherical cap grid shells, the effect of grid size grid shape and span to depth ratio on buckling load has been studied. For corrugated barrel vault grid shells, the effect of corrugation has been studied. Different equivalent models have been used to establish equivalency between grid shell and equivalent continuous shell. Expression for buckling of the continuous shell has been used to determine the buckling load of grid shells analytically. A 2D Arch analysis is prepared to establish the accuracy of FEM. Linear buckling analysis has been done for analysis parameters. It has been concluded that:

- A triangular grid is better for steeper shells (spherical cap).
- A denser grid is recommended for the shallower shell.
- Buckling load decreases with increases in grid size and shallowness.
- Corrugation improves the load-carrying capacity of barrel vaults.
- The equivalent area model gives a conservative estimate of the buckling load of the grid shell.

CHAPTER 4: METHODOLOGY

This chapter illustrates the methodology for the progress of this thesis. The methodology is oriented towards the fulfilment of the objectives of this thesis. A process is established from previous works done, to answer some of the research questions and problems in grid shells mentioned in Chapter 1.3

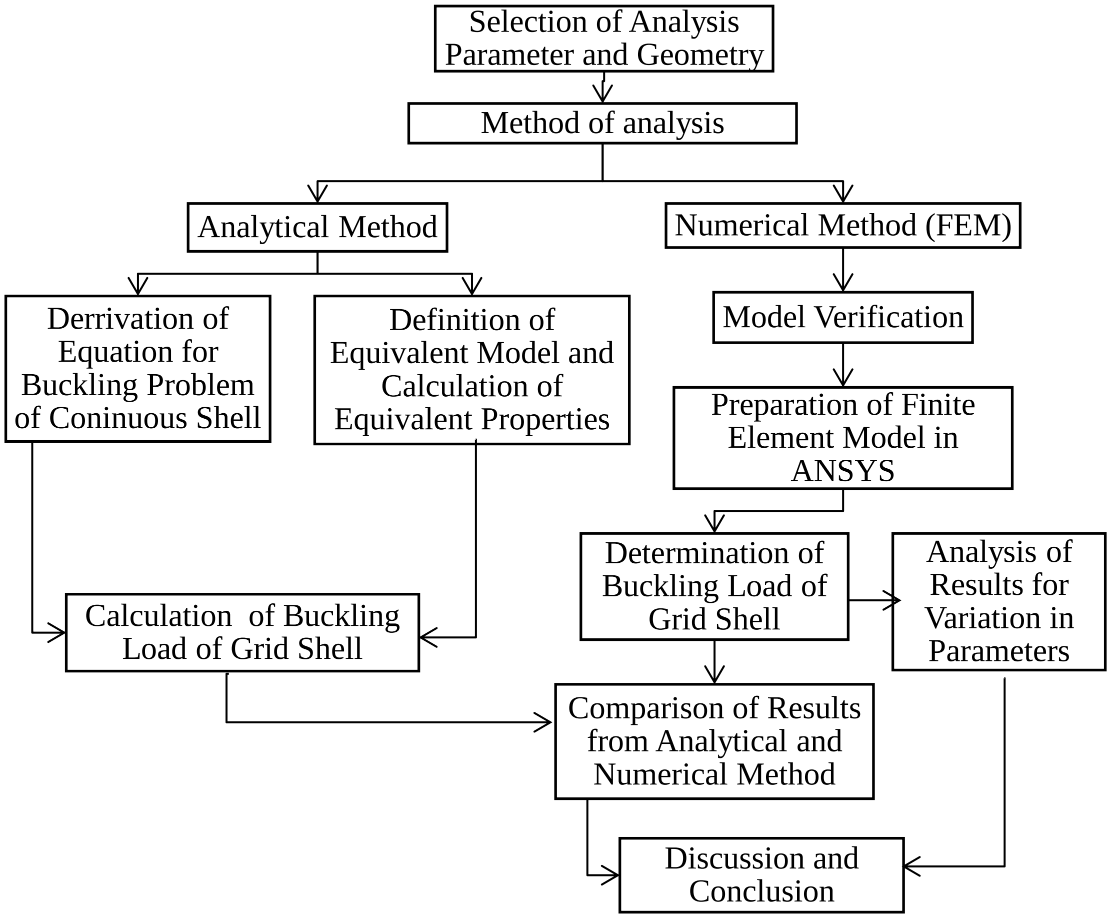

Figure 4.1: Flowchart of methodology

4.1 Procedure for Parametric Analysis

The parameters required for analysis has been deduced from the literature review in Chapter 1.4. The numerical value of parameters for analysis is identified from previously built grid shells. An insight on analysis methods, their usefulness and limitations are very necessary.

4.1.1 Selection of analysis parameters

In the recent decade, several grid shell structures have been constructed around the world. The structures are built individually as per requirement. Various materials (from steel to cardboard) and geometries have been used. These grid shells have varying values and a combination of parameters. Some grid shells with their parameters are given in Table 4.2 (Mesnil, 2013) (Schober, 2015).

In the construction of grid shells, a quadrilateral grid has been used mainly which is easier to construct. But for aesthetic requirements triangular grid has also been used. The size of the grid varies from 500mm to 2000mm. A grid cannot be too fine and use short elements because it would use more material and would not fulfil the required functionality. Also, the grid should not be too coarse and use slender elements because it would invite local instability. As the member length is shorter than buckle wavelength, the member axial load is well below the Euler buckling load of simply supported column (Forman & Hutchinson, 1970). It enables the use of an equivalent continuum approach.

The span to depth ratio indicates the shallowness or steepness of the grid shell. Span to depth ratios (r) of 5, 14, 20 are chosen for analysis as a representative value of previously built grid shells and shallowness of shell. Quadrilateral and triangular grid with grid size(s) of 500mm, 1000mm & 1500mm is selected. Grid element (rod) made of steel (E = 210GPa, ν = 0.3) with solid cross-section of 50mm x 50mm is selected for analysis. Open circular-cylinder geometry is chosen for analysis. Other factors required to define geometry are mentioned in Chapter 5.2. The analysis parameters and grid element properties are summarized in Table 4.1.

Table 4.1: List of properties of grid shell and analysis parameters

Global Geometry	Open circular-cylindrical
Span to depth ratio (r)	5, 14, 20
Grid Shape	Quadrilateral & Triangular (Single Layered)
Grid Size/Spacing of grid element (s)	500mm, 1000mm, 1500mm
Grid element (rod) Size	50mm x 50mm
Cross-Section Area of grid element (A)	2500mm^2
Moment of Inertia of grid element (I)	5.208 x 10^{5}mm^4
Torsional Moment of Inertia of grid element (J)	8.813 x 10^{5}mm^4
Modulus of Elasticity (E)	210000 N/mm^2
Poission`s ratio (ν)	0.3
Modulus of Rigidity (G)	80769.23 N/mm^2

Table 4.2: Some grid shells with their parameters

Grid Shell	Year	Location	Span (m)	Rise (m)	Span/Rise	Grid Shape	Grid Size(m)	Element Size(mm)	Material
Mannheim Multihalle	1975	Mannheim, Germany	55 x 55	15.5	3.55	Quadrilateral	0.5 x 0.5	50 x 50	Timber
Museum for Hamburg History	1989	Hamburg, Germany	50 x 17	5	3.4	Quadrilateral	1.17 x 1.17	60 x 40	Steel
Swimming Arena Neckarsulm	1989	Neckarsulm, Germany	25.2	5.75	4.38	Quadrilateral	1.0 x 1.0	60 x 40	Steel
Railway station Berlin	1998	Berlin, Germany	18 x 9.7	3.8	2.55	Quadrilateral	1.5 x 1.2	60 x 60	Steel
Yas Mall, Atrium roof	2013	Abu Dhabi, UAE	29 x 52	3.52	14.77	Quadrilateral	2.18 x 2.15	80 x 160	Steel (Hollow Sections)
Cabot Circus	2007	Bristol, UK	40/60		5.26	Quadrilateral	1.5 x 1.75	60 x 80	Steel
Weald and Downland Museum	2002	West Sussex, UK	16.5	9.5	1.74	Triangular	1.0 x 1.0	50 x 35	Timber

4.1.2 Method of Analysis

The basic process of solving a problem is identification, formulation and solution. The formulation can be done either by assessing the properties and constraints of the problem and preparing a model for each problem differently or by fitting an existing solution to a problem with some assumptions. The succeeding approach is applied here for the analytical solution. A discrete (grid) shell is idealized as a continuous shell establishing some equivalence. Results for the continuous shell are applied to the discrete shell with those equivalencies and final solutions are regarded as grid shell.

In engineering, every problem may not result in a closed-form solution. With increasing complexity in the idealization and formulation of a problem, an exact solution becomes less feasible. Numerical methods are applied for those problems whose exact solutions are not available. FEM is a common tool for solving such complex problems. Finite element models are prepared for each combination of parameters mentioned in Chapter 4.1.1 and results are compared with the analytical solution. A 2D-Arch analysis is prepared using FEM and the method is validated by comparing the results from the exact analytical solution.

4.2 Analytical Method

In this thesis, an equivalent continuous shell is defined for grid shell to solve the problem analytically. A shell has to transfer the load either by membrane action or by bending action or by a combination of them. The load transfer characteristics are defined by its axial (membrane) or bending rigidity. The thickness has to be decided based on the trade-of of whether the shell has to transfer load by membrane action or bending action. C and D are the axial and bending rigidity which are given in Eq. 4.1 & Eq. 4.2 respectively.

$$C = \frac{Eh}{(1 - \upsilon^2)} \qquad \text{Eq. 4.1}$$

$$D = \frac{Eh^3}{12(1 - \upsilon^2)} \qquad \text{Eq. 4.2}$$

A relationship between the element of grid shell (rod) and shell`s axial and flexural rigidities is defined using methods illustrated in Chapter 2.1. An equivalent thickness and modulus of elasticity are defined for a continuous shell.

4.2.1 Equivalent Volume Model

In this model, it is idealized that a volume can be deformed into a continuous and reticulated shell. The volume of rods at the boundary is neglected and the volume of intersection of the rod is counted twice. There is a very low error between the volume between the grid shell and its equivalent continuous shell.

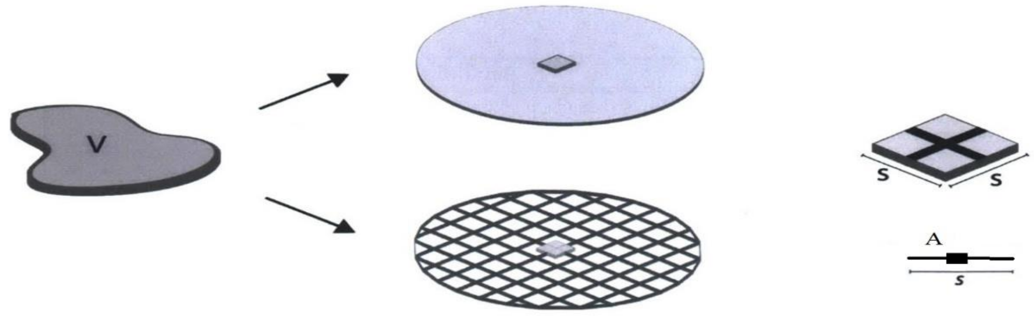

Figure 4.2: Equivalent volume model

$$V_{continious\ shell} = V_{rod} \quad \text{Eq. 4.3}$$

For quadrilateral grid;

$$2As = h_{eq}s^2$$

$$h_{eq} = \frac{2A}{s} \quad \text{Eq. 4.4}$$

For triangular grid;

$$h_{eq} = \frac{8A}{\sqrt{3}s} \quad \text{Eq. 4.5}$$

4.2.2 Equivalent Area Model

In this model, the cross-section area of a rod of the grid shell is taken as equivalent to the cross-section area of the continuous shell. The equivalent area represents the membrane characteristics of the grid shell.

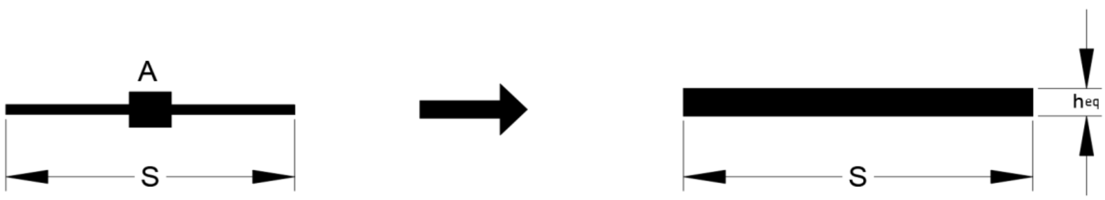

Figure 4.3: Equivalent area model

$$A_{rod} = A_{continious\ shell} \quad \text{Eq. 4.6}$$

For quadrilateral grid;

$$As = h_{eq}s^2$$

$$h_{eq} = \frac{A}{s} \quad \text{Eq. 4.7}$$

For triangular grid;

$$h_{eq} = \frac{2A}{s} \quad \text{Eq. 4.8}$$

4.2.3 Equivalent Moment of Inertia Model

In this model moment of inertia of a rod of the grid, the shell is taken as equivalent to the moment of inertia of cross-section of the continuous shell. Area and moment of inertia give the bound between axial and bending characteristics of grid shell.

$$MOI_{rod} = MOI_{continious\ shell} \quad \text{Eq. 4.9}$$

For quadrilateral grid;

$$I = \frac{sh_{eq}^3}{12}$$

$$h_{eq} = \left(\frac{12I}{s}\right)^{1/3} \quad \text{Eq. 4.10}$$

For triangular grid;

$$h_{eq} = \left(\frac{24I}{s}\right)^{1/3} \quad \text{Eq. 4.11}$$

4.2.4 Split Rigidity Model

In this model both axial and bending rigidities are defined for an equivalent continuous shell. Considering the homogenized models (Mesnil, et al., 2017) has given rigidities for an equivalent continuous shell.

For quadrilateral grid;

$$C_{eq} = \frac{EA}{s}$$

$$D_{eq} = \frac{EI}{s} \quad \text{Eq. 4.12}$$

For triangular grid

$$C_{eq} = \frac{2EA}{s}$$
$$D_{eq} = \frac{2EI}{s} \qquad \text{Eq. 4.13}$$

4.2.5 Orthotropic Equivalence Model

Pshenichnov (1993) has derived a set of the equation for the orthotropic shell from the anisotropic shell and has used a constitutive equation for an element of grid shell (rod) to derive the expressions for forces and moments of the equivalent continuous shell. The equivalent properties of the grid shell are given in Eq. 4.14 and Eq. 4.15.

For quadrilateral grid (two families of the rod, n=2);

$$C_{eq} = \frac{EA}{s}, \nu_c = 0$$
$$D_{eq} = \frac{EI}{s}, \nu_D = 0 \qquad \text{Eq. 4.14}$$

For triangular grid (three families of the rod, n=3);

$$C_{eq} = \frac{9EA}{8s}, \nu_c = \frac{1}{3}$$
$$D_{eq} = \frac{3EI(1+\gamma)}{8s}, \nu_D = \frac{1-\gamma}{3+\gamma} \qquad \text{Eq. 4.15}$$
$$\gamma = \frac{GJ}{EI}$$

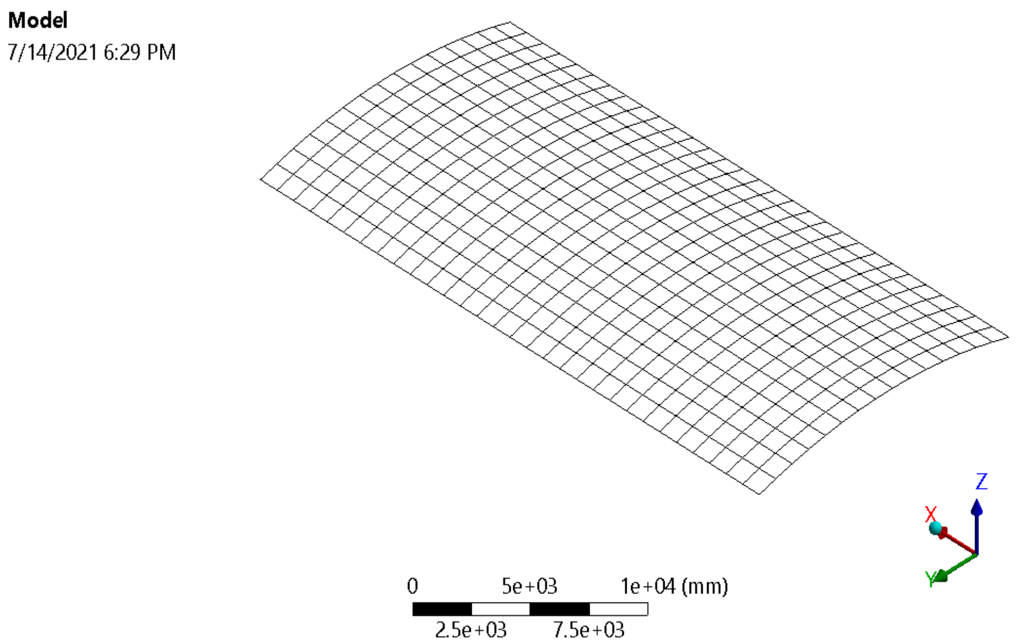

Figure 4.4: Undeformed grid shell (Quadrilateral grid r=14, s=1000)

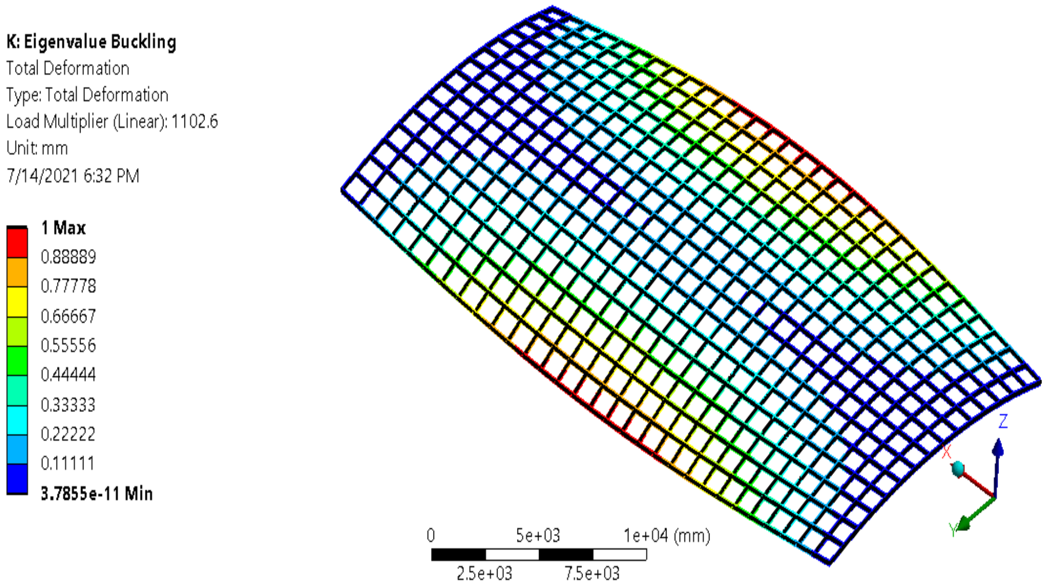

Figure 4.5: Deformed grid shell (Quadrilateral grid r=14, s=1000)

4.3 Numerical Method

The finite element formulation of buckling problem of beam element can be described in Eq. 4.16 and Eq. 4.17 (Zienkiewicz & Taylor, 2005)

$$[K_E]\{Q\} = \{F\} \qquad \text{Eq. 4.16}$$

$$\left[[K_M] - \lambda_n[K_G]\right]\{Q_n\} = \{0\} \qquad \text{Eq. 4.17}$$

Where, $[K_E]$ is stiffness matrix, $\{Q\}$ is displacement vector and $\{F\}$ is load vector for linear force analysis. Solving Eq. 4.16, forces in each element can be calculated which is given by $[T_i]$. $[K_M], [K_G], \{Q_n\}$ and λ_n are stiffness matrix for large displacement, geometric stiffness matrix, displacement vector of n^{th} mode and load factor of n^{th} mode respectively which are given in Eq. 4.18.

$$[K_G] = \sum_i [\,[L_i]^T (\int_0^l [N`]^T [T_i][N`]dx)[L_i]]$$
$$[K_M] = \sum_i [\,[L_i]^T (\int_0^l [B_a]^T [D_T][B_a]dx)[L_i]] \qquad \text{Eq. 4.18}$$

Where, $[N]$ is shape function, $[B_a]$ is the strain-displacement relationship for large displacement and $[D_T]$ is elastic relationship. Eq. 4.17 can be solved as an eigenvalue problem $(|[K_M] - \lambda_n[K_G]| = 0)$ and load factor λ_n can be determined. Multiplying applied load by the load factor, buckling load is determined.

For this thesis, test geometries for analysis are created in Rhino 6 using the Grasshopper plugin. The geometries are imported in ANSYS Workbench 2020 R1 and a finite element analysis model is prepared with properties given in Table 4.1. Linearized buckling analysis is prepared and numerical results are compared with analytical results.

Table 4.3: Summary of equivalent models and equivalent properties

Equivalent Model	Equivalent Properties					
	Quadrilateral Grid			Triangular Grid		
	h_{eq}	C_{eq}	D_{eq}	h_{eq}	C_{eq}	D_{eq}
Equivalent Volume	$\frac{2A}{s}$	$\frac{Eh_{eq}}{(1-\upsilon^2)}$	$\frac{Eh_{eq}^3}{12(1-\upsilon^2)}$	$\frac{8A}{\sqrt{3}s}$	$\frac{Eh_{eq}}{(1-\upsilon^2)}$	$\frac{Eh_{eq}^3}{12(1-\upsilon^2)}$
Equivalent Area	$\frac{A}{s}$	$\frac{Eh_{eq}}{(1-\upsilon^2)}$	$\frac{Eh_{eq}^3}{12(1-\upsilon^2)}$	$\frac{2A}{s}$	$\frac{Eh_{eq}}{(1-\upsilon^2)}$	$\frac{Eh_{eq}^3}{12(1-\upsilon^2)}$
Equivalent Moment of Inertia	$\left(\frac{12I}{s}\right)^{\frac{1}{3}}$	$\frac{Eh_{eq}}{(1-\upsilon^2)}$	$\frac{Eh_{eq}^3}{12(1-\upsilon^2)}$	$\left(\frac{24I}{s}\right)^{\frac{1}{3}}$	$\frac{Eh_{eq}}{(1-\upsilon^2)}$	$\frac{Eh_{eq}^3}{12(1-\upsilon^2)}$
Split Rigidity		$\frac{EA}{s}$	$\frac{EI}{s}$		$\frac{2EA}{s}$	$\frac{2EI}{s}$
Orthotropic Equivalence		$\frac{EA}{s}$, $\nu_c = 0$	$\frac{EI}{s}$, $\nu_D = 0$		$\frac{9EA}{8s}$, $\nu_c = \frac{1}{3}$	$\frac{3EI(1+\gamma)}{8s}$, $\nu_D = \frac{1-\gamma}{3+\gamma}$ $\gamma = \frac{GJ}{EI}$

4.4 Model Verification and 2D Arch Analysis

For the validation of a more complicated computational modelling technique required for grid shell, simpler failure mode and buckling mode of 2D Arch is analyzed. 2D Arch is a proper prototype to test various methods and approximations for the study of grid shells. 2D Arch shows an interplay between bending and membrane action. Malek (2012) and Mesnil (2013) has used 2D Arch analysis for verifying modelling techniques.

4.4.1 Buckling Load Convergence

Timoshenko and Gere (1985) has given expression for buckling load for a circular arch under normal loading which is given in Eq. 4.19.

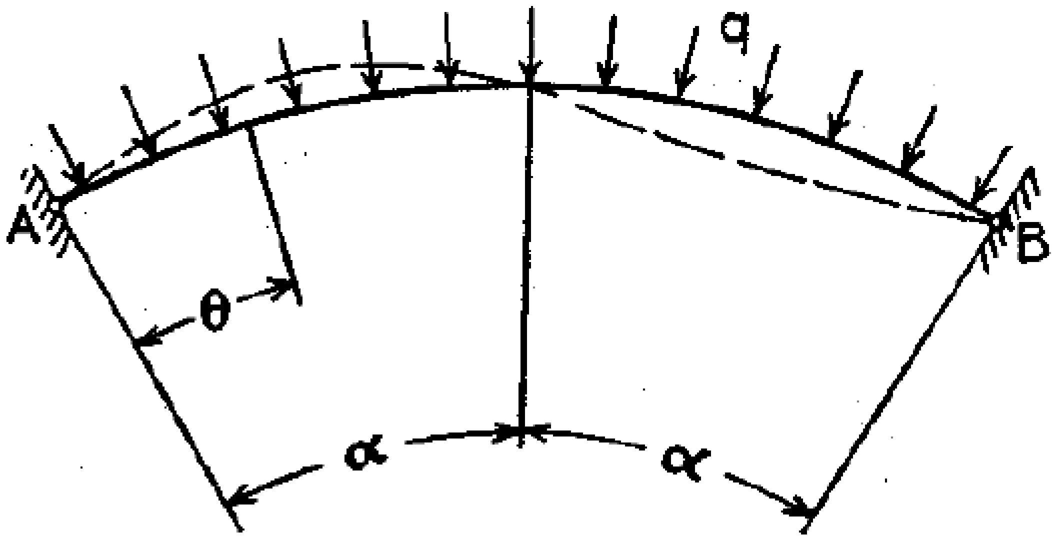

Figure 4.6: 2D Arch geometry

$$q_c = \frac{EI}{R^3}\left(\frac{\pi^2}{\alpha^2} - 1\right) \qquad \text{Eq. 4.19}$$

For 2D Arch, it has been established that for span/depth≤20 the mode of failure is due to buckling. For verifying the accuracy of FEM both buckling load convergence and load equivalency are checked. An arch of span 15000mm, span to depth ratio 5, 14 & 20 and properties similar to grid element (rod) are taken for analysis. Both analytical and finite element analysis results are compared and the accuracy of FEM is established. The results are shown in Table 4.4. Applying normal load to an arch in ANSYS Workbench is not possible so instead vertical load is applied. As the arch becomes shallow, the difference between vertical and normal load becomes smaller and the error between analytical and finite element results becomes smaller.

Table 4.4: Comparison of the buckling load of 2D Arch

Geometric Properties				Buckling Load(q_c)(N/mm)		Error
Span(L) (mm)	Span to depth ratio (r)	Radius (R)(mm)	Angle(α) (rad)	Analytical	FEM	%
15000	5	10875	0.761013	1.364E+00	1.238E+00	9.281
15000	14	26785.71	0.283794	6.917E-01	6.617E-01	4.346
15000	20	37875	0.199337	4.980E-01	4.873E-01	2.149

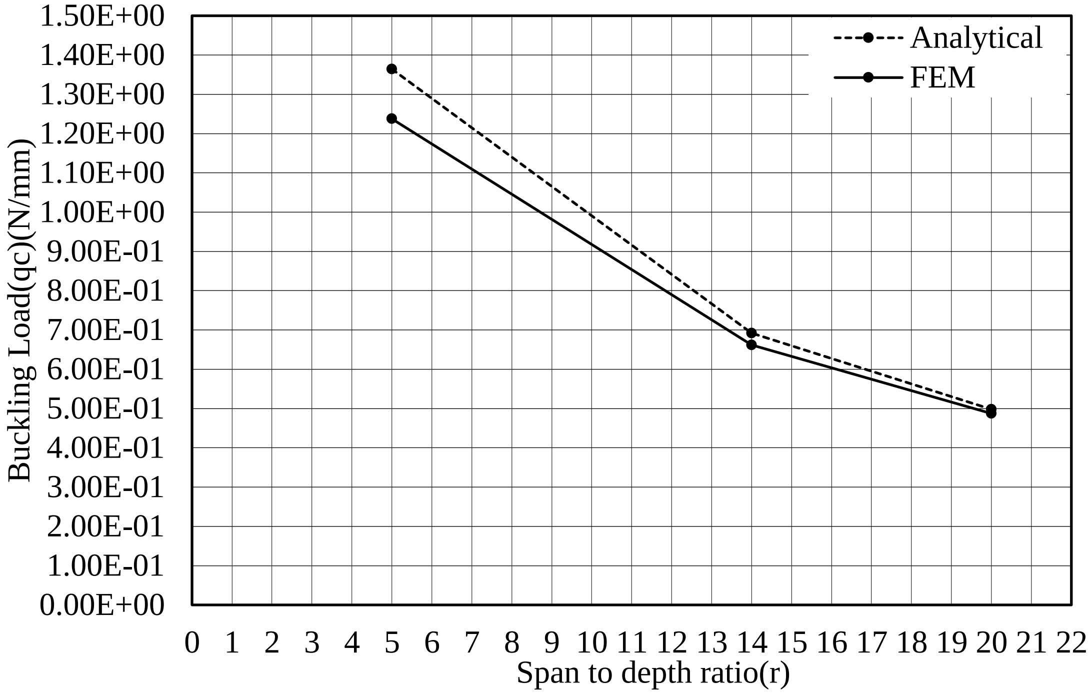

Figure 4.7: Comparison of the buckling load of 2D Arch

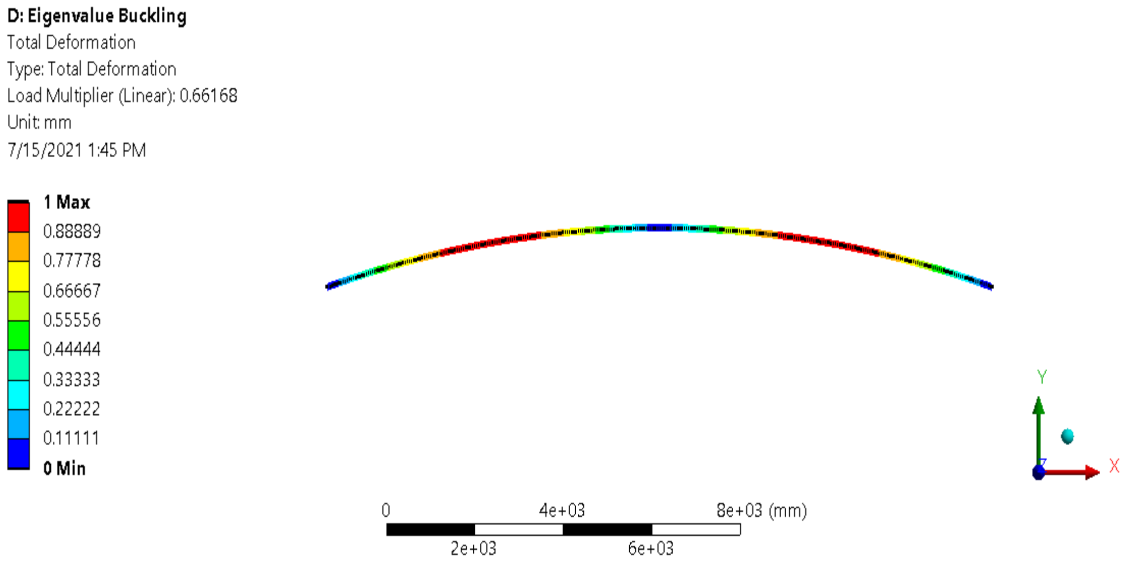

Figure 4.8: The deformed shape of the arch (r=14)

The maximum error between analytical and FEM results is 9.281% for r=5 and reduces with the reduction in the value of r. The error is also due to applied vertical load instead of normal load. But in the case of grid shell, a normal load can be applied.

4.4.2 Load Equivalency

In an analytical solution of 2D Arch, the load applied is linear pressure load. But for grid shells, the load applied is point load at joints. So, it is necessary to establish that analytical solution assuming pressure load can be used for grid shells when the applied load is point load at joints. If P is point load, N is no. of node and S is the arc length of the arch then buckling load can be determined from Eq. 4.20.

$$q_c = \frac{PN}{S} \qquad \text{Eq. 4.20}$$

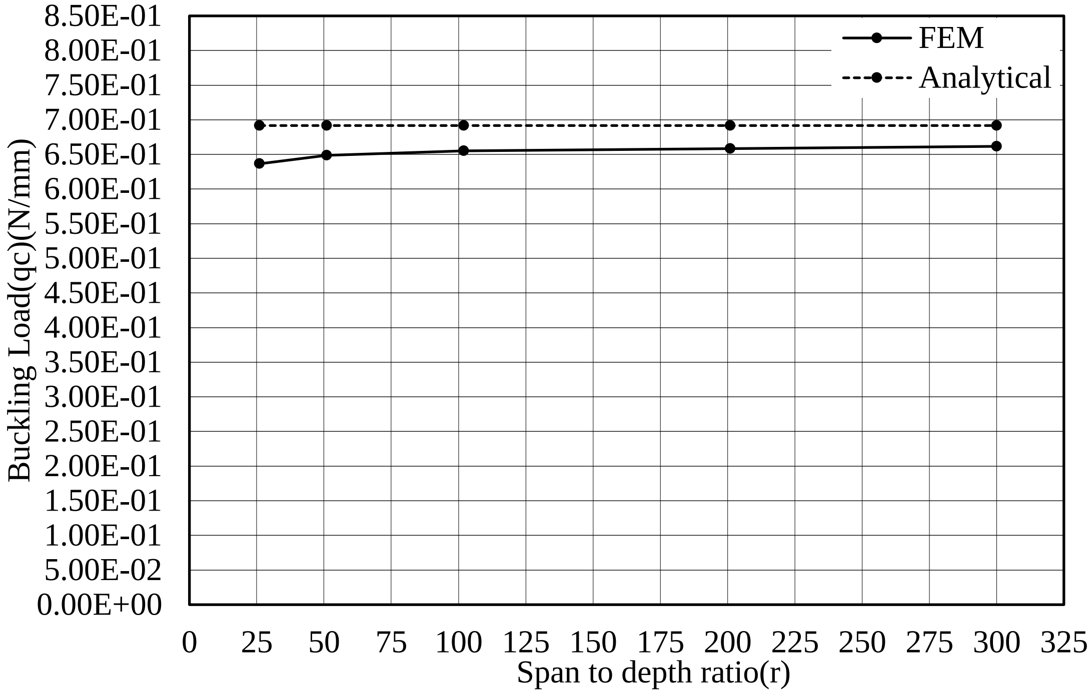

Figure 4.9: Load equivalence for the arch (r=14)

For arch of r=14, the error between the analytical result and FEM result is 4.35% with 300 elements. The result also shows FEM results for both pressure load and point load are almost the same.

CHAPTER 5: PARAMETRIC STABILITY ANALYSIS

5.1 Introduction

Grid shells have various advantages which are illustrated in Chapter 1.2. A circular-cylindrical grid shell has simpler geometry and omits many complexities in construction due to geometry. Previous literature in Chapter 3 has stated that the failure mode of the grid shell is buckling. This chapter illustrates both the analytical method and FEM to calculate the buckling load of the grid shell. Buckling load in sense of strength is understood as the load-carrying capacity of grid shells.

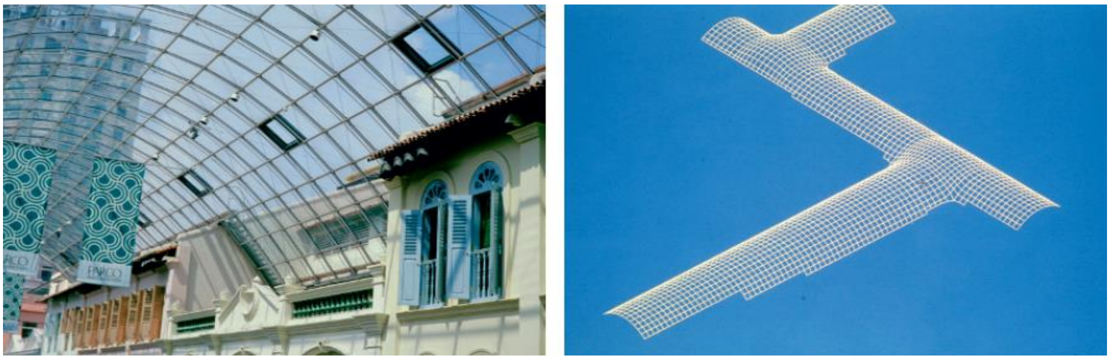

Figure 5.1: Roof Bugis Street Singapore (Schober, 2015)

5.2 Analysis Parameters

An open circular-cylindrical grid shell with span (L) 15000mm and length (l) 30000mm is considered for analysis. Other analysis parameters are given in Table 4.1.

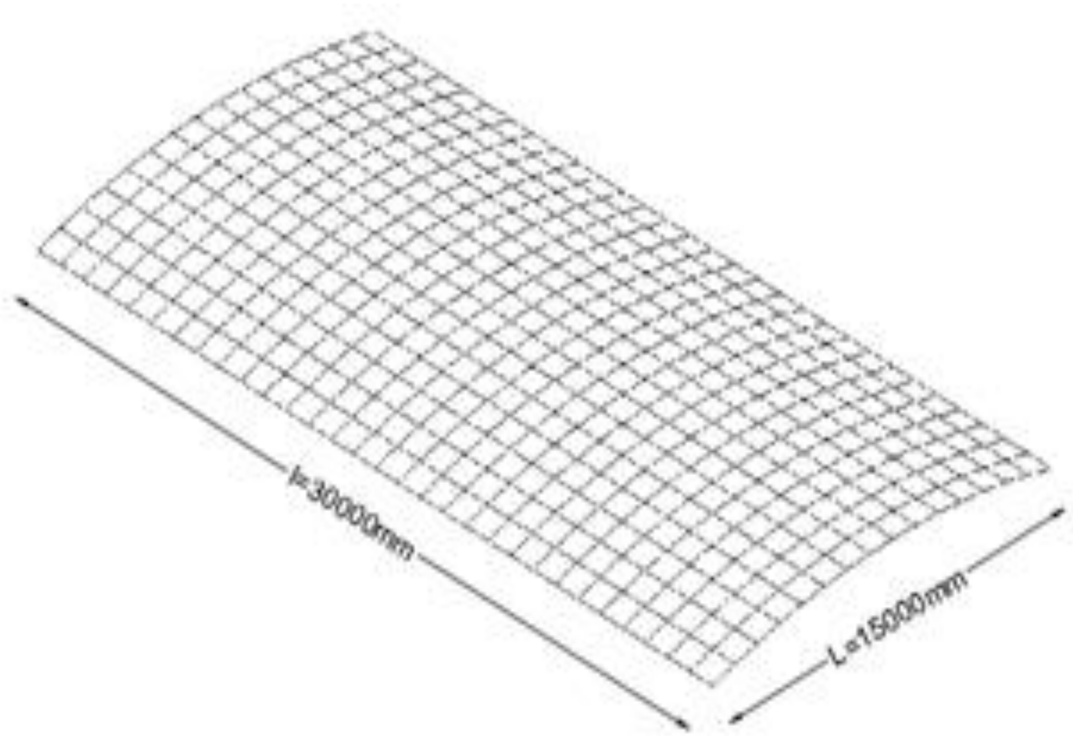

Figure 5.2: Geometric property of grid shell

5.3 Analytical Method

The equivalent continuum approach is used to determine the buckling load of the grid shell analytically. Various continuum models are illustrated in Chapter 4.2. equivalent properties (C_{eq}, D_{eq}, ν_c & ν_D) are calculated by a program written in MATLAB. Equivalent properties are calculated for quadrilateral and triangular grids with variation in grid size as other parameters are constant in this analysis. Parameters ϕ and α in Eq. 2.7 is determined as $\phi = \frac{qa}{C_{eq}}$ and $\alpha = \frac{D_{eq}}{C_{eq}a^2}$ and modified equation is the governing equation for buckling problems. Buckling load of grid shell is determined by solving modified Eq. 2.7 with equivalent properties and span to depth ratio as an input parameter. A program in MATLAB is written to calculate the buckling load of grid shells analytically as a matrix of grid size and continuum model for each value of span to depth ratio. The final results are presented as graphical plots of buckling load vs grid size for each value of span to depth ratio. Source code for the program in MATLAB is given in Chapter A.2.

5.4 Numerical Method

For finite element analysis, geometries are generated in Rhino6 & Grasshopper with a maximum length error of 1.9% for the quadrilateral grid and 7.8% for the triangular grid. 18 geometrical models are created for analysis parameters, and visual code for geometry generation is given in Chapter A.3. The geometries are imported in ANSYS SpaceClaim and models for further analysis are created. The element of grid shell (rod) is modelled as beam element in ANSYS Material properties & cross-section is assigned and mesh is generated with an element size of 50mm. Point force is applied at vertices (joints) in radial (normal) direction and simply supported boundary condition is applied. Linear buckling analysis is performed to calculate the buckling load of the grid shell.

5.5 Analysis Results

5.5.1 Model Verification

To proceed for further analysis, it becomes necessary to verify the analytical validity of the equation derived to calculate buckling load of continuous shell and source code written for calculating buckling load of grid shell. Also, the accuracy of FEM in solving buckling problems is established. 6 models of the continuous shell with different thicknesses are prepared in ANSYS and buckling loads of respective models are determined. Parameters and results are presented in Table 5.1.

Table 5.1: Parameters and results for continuous shell

Geometric Properties							Buckling Load(q_c)(N/mm^2)		Error
Grid Shape	Grid Size(s) (mm)	Span(L) (mm)	Length(l) (mm)	Span to depth ratio(r)	Equivalent Model	Equivalent Thickness(h_{eq}) (mm)	Analytical	FEM	%
Quadrilateral	1000	15000	30000	5	Eq. Volume	5	3.196E-04	3.200E-04	0.12
Quadrilateral	1000	15000	30000	14	Eq. Area	2.5	1.464E-05	1.473E-05	0.55
Quadrilateral	1000	15000	30000	20	Eq. MOI	18.4202	1.319E-03	1.324E-03	0.37
Triangular	1000	15000	30000	5	Eq. Volume	11.547	2.594E-03	2.604E-03	0.4
Triangular	1000	15000	30000	14	Eq. Area	5	8.316E-05	8.349E-05	0.39
Triangular	1000	15000	30000	20	Eq. MOI	23.2079	2.358E-03	2.365E-03	0.29

The model uses shell elements and the maximum error between analytical and finite element results is 0.55% for the first buckling mode. Because the corresponding buckling load has only 0.55% error from the analytical result this error is negligible.

5.5.2 Analytical Results

Buckling load of grid shell calculated analytically is presented as the graphical plot in Figure 5.3 to Figure 5.8. The graphical plots clearly show that the equivalent MOI model and equivalent area model gives an upper and lower bound of the behaviour of grid shell except for small grid size for the triangular grid. But for practical purposes, a small grid size is not desired.

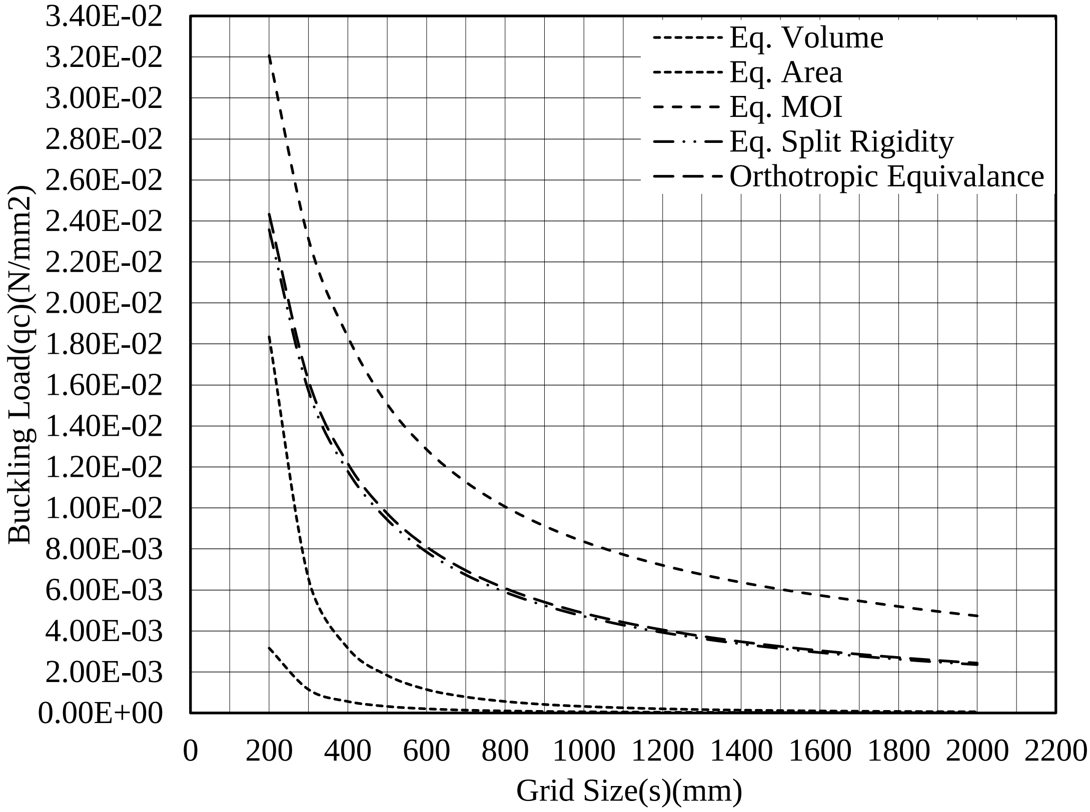

Figure 5.3: Analytical buckling load of grid shell (Quadrilateral grid, r=5)

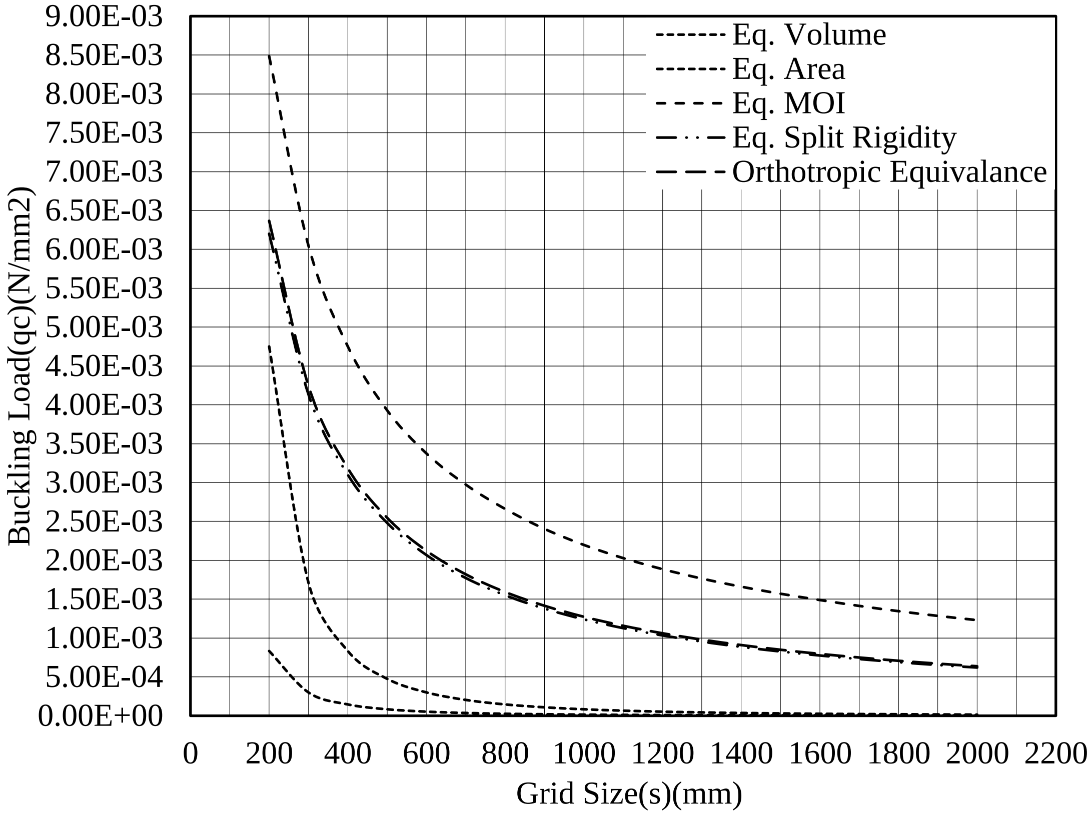

Figure 5.4: Analytical buckling load of grid shell (Quadrilateral grid, r=14)

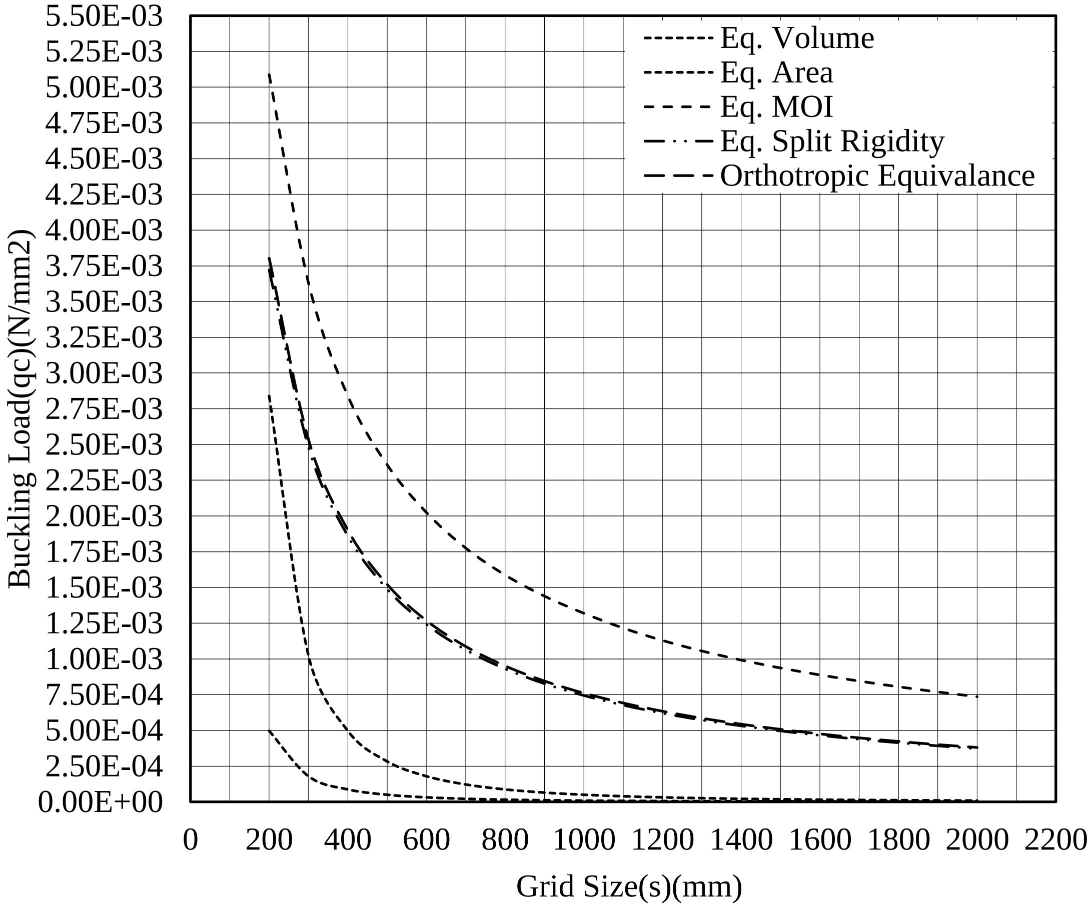

Figure 5.5: Analytical buckling load of grid shell (Quadrilateral grid, r=20)

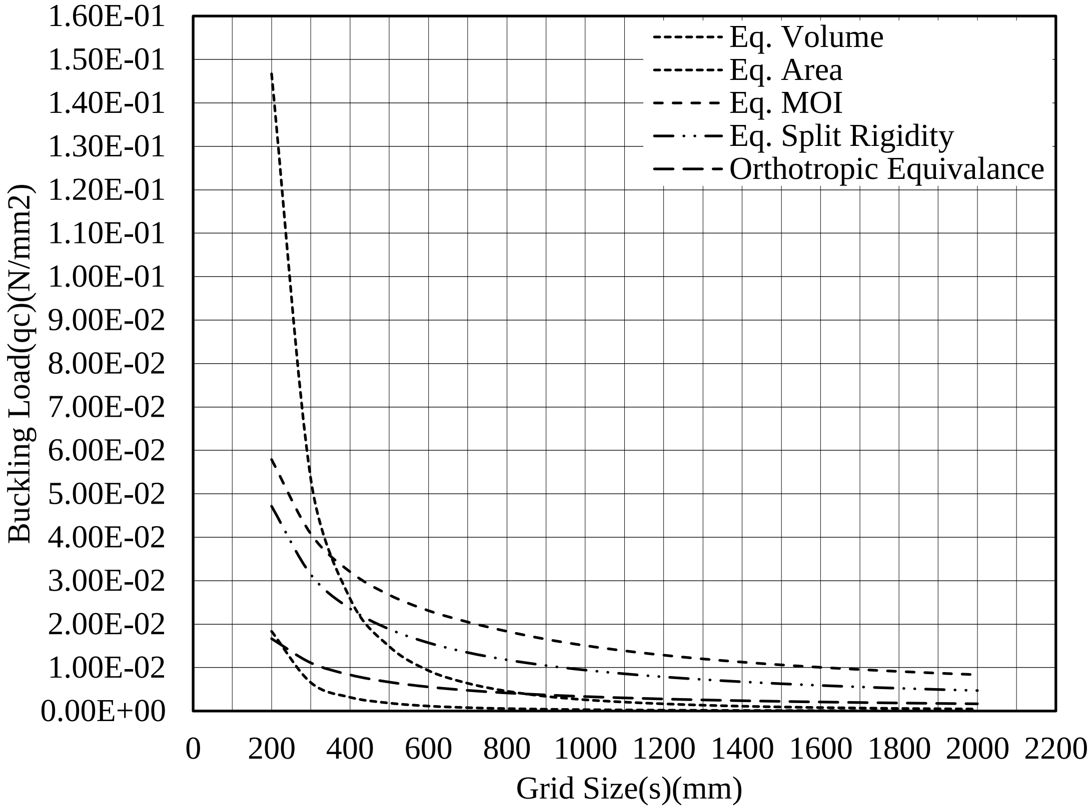

Figure 5.6: Analytical buckling load of grid shell (Triangular grid, r=5)

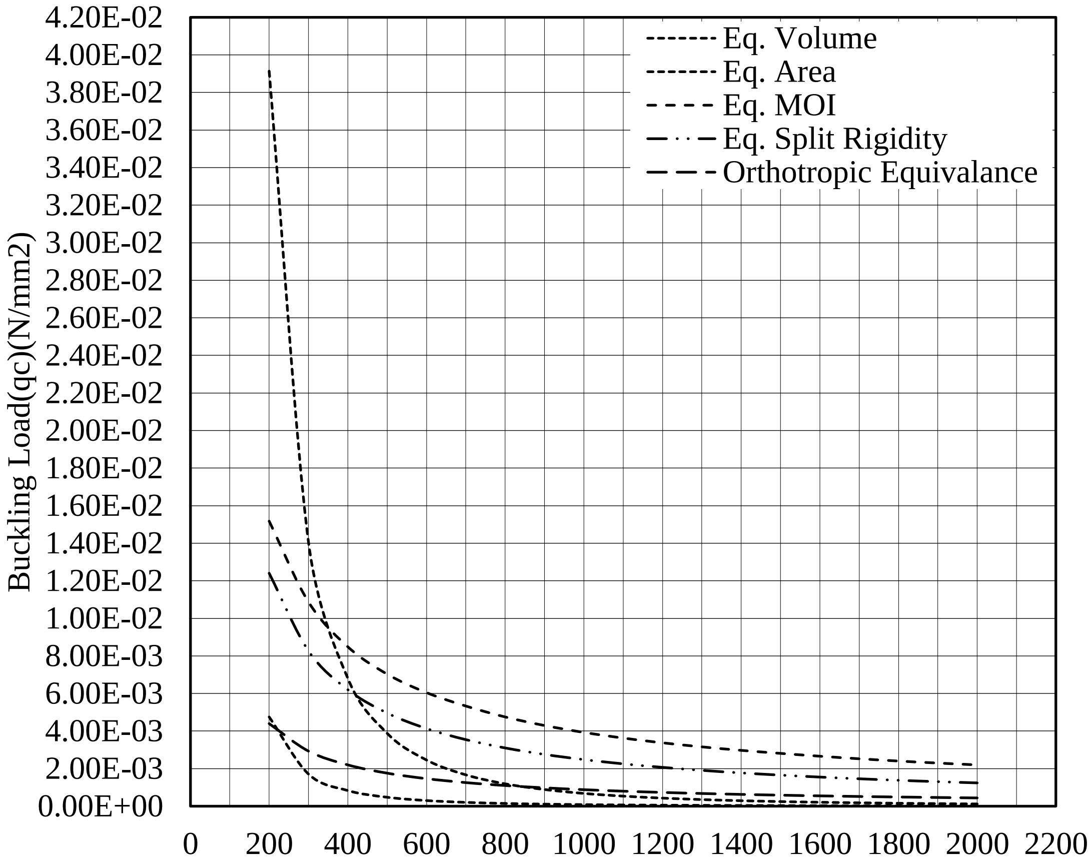

Figure 5.7: Analytical buckling load of grid shell (Triangular grid, r=14)

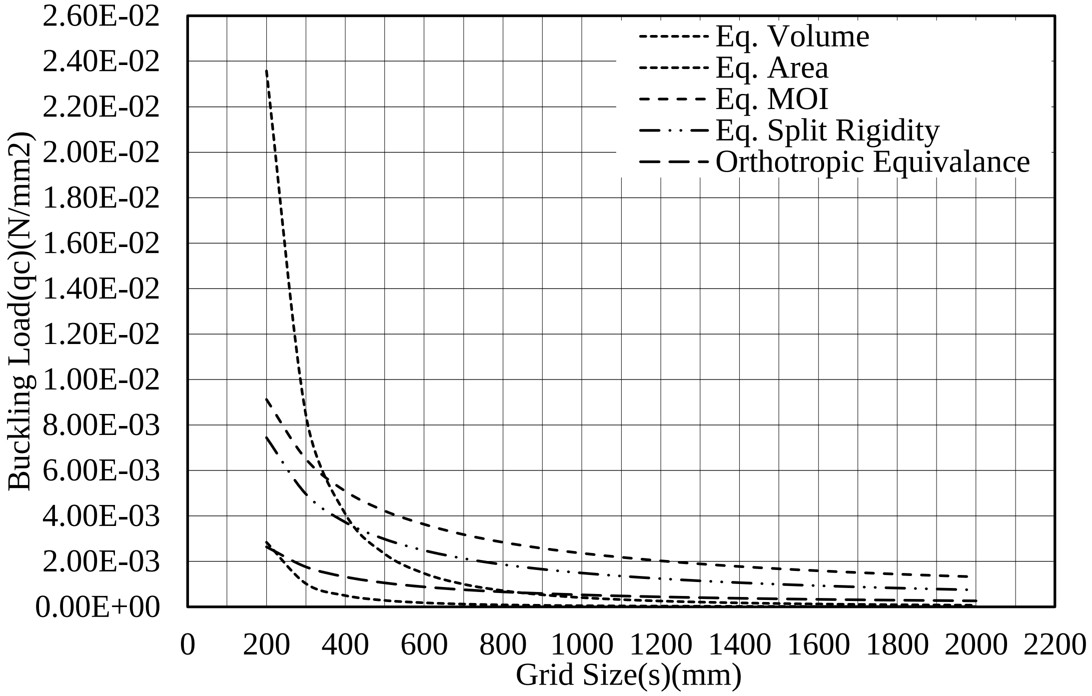

Figure 5.8: Analytical buckling load of grid shell (Triangular grid, r=20)

5.5.3 Numerical Results

The objective of this thesis is to study the change in load-carrying capacity of grid shells as a function of grid type, grid size and span to depth ratio. The output of finite element analysis is presented in Figure 5.9 and Figure 5.10.

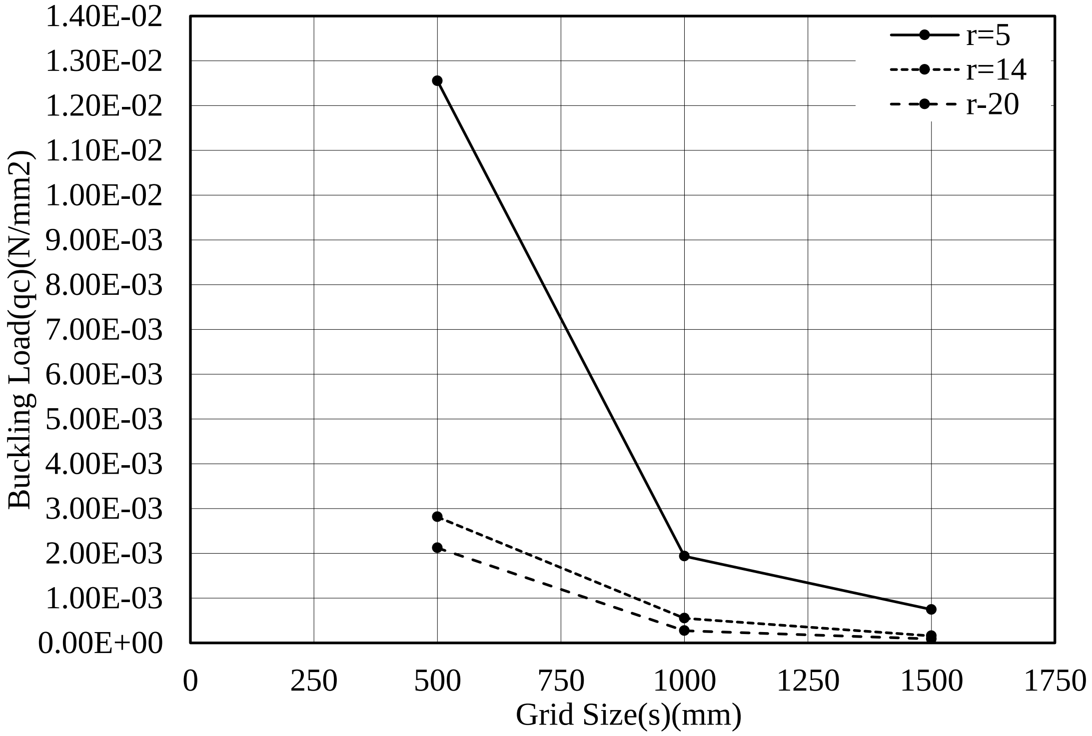

Figure 5.9: Numerical buckling load of grid shell (Quadrilateral grid)

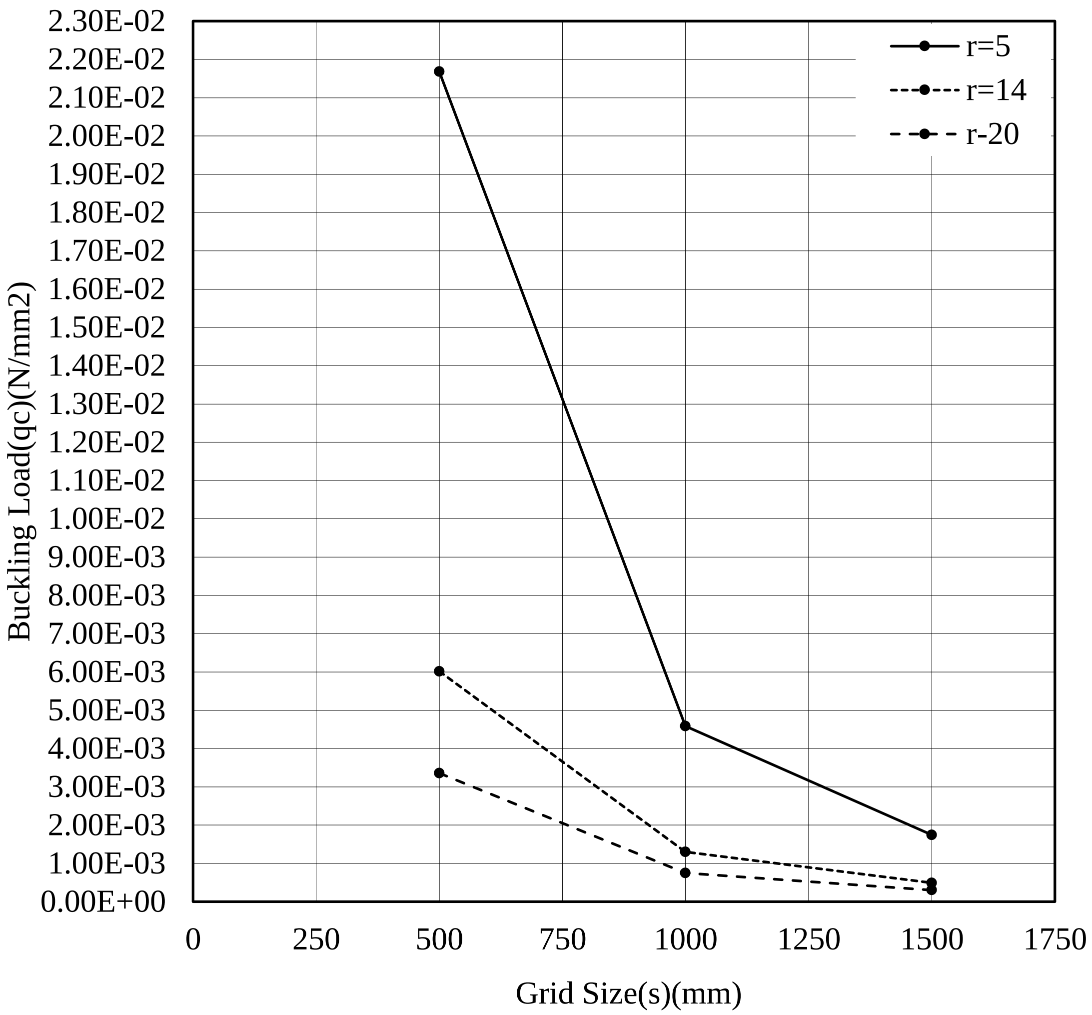

Figure 5.10: Numerical buckling load of grid shell (Triangular grid)

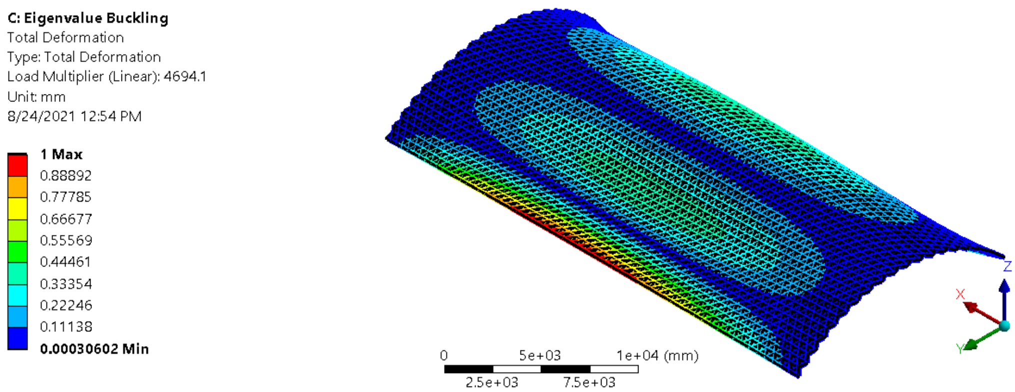

Figure 5.11: The deformed shape of grid shell (Triangular grid r=5, s=500)

Buckling load as uniform pressure is calculated as $q_c = \frac{Point\ load}{Area(s^2)}$. The result of finite element analysis clearly shows the buckling load of the grid shell reduces significantly with an increase in grid size. Considering the effect of span to depth ratio, the shallower shell has less buckling load. Increasing span to depth ratio from 5 to 14 buckling load reduces rapidly. The load-carrying capacity for the triangular grid is 2 to 3 times more than the quadrilateral grid.

5.5.4 Comparison of Analytical and Numerical Result

From Figure 5.12 to Figure 5.17 plots both numerical and analytical results for all values of span to depth ratio for the quadrilateral and triangular grid.

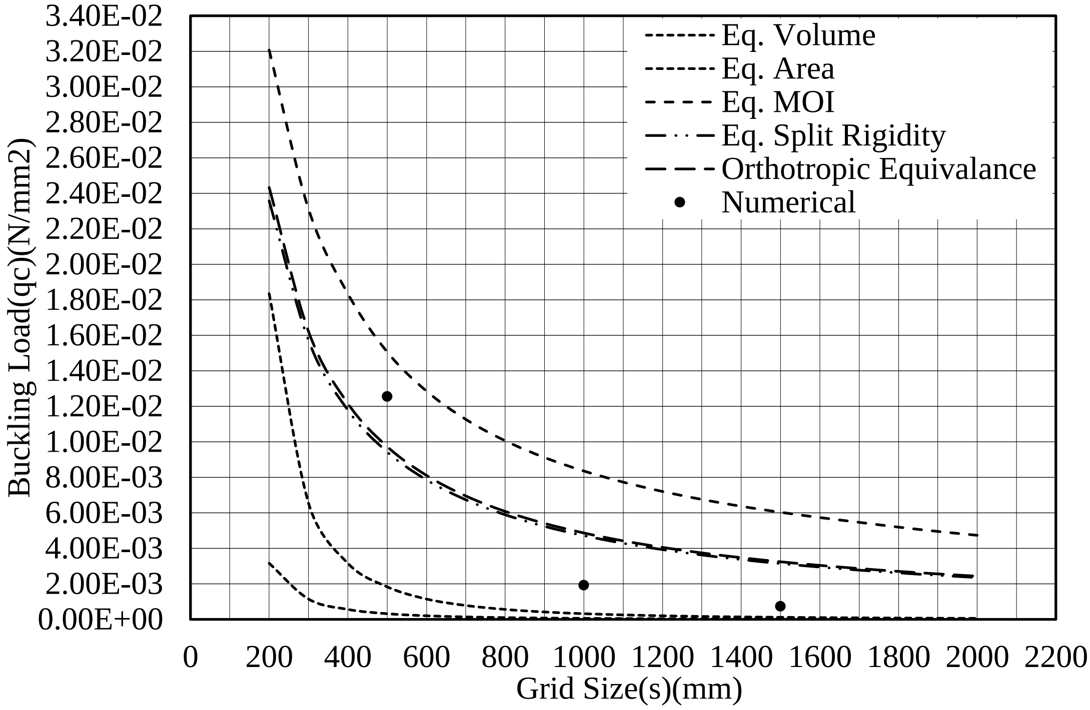

Figure 5.12: Comparison of buckling load (Quadrilateral grid, r=5)

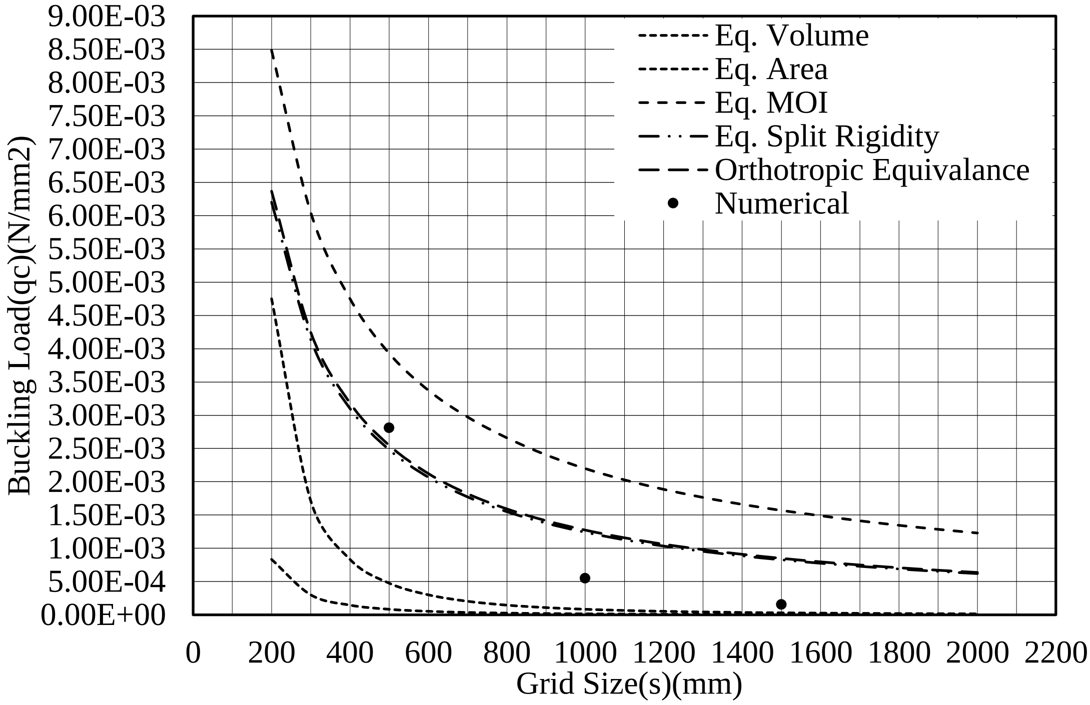

Figure 5.13: Comparison of buckling load (Quadrilateral grid, r=14)

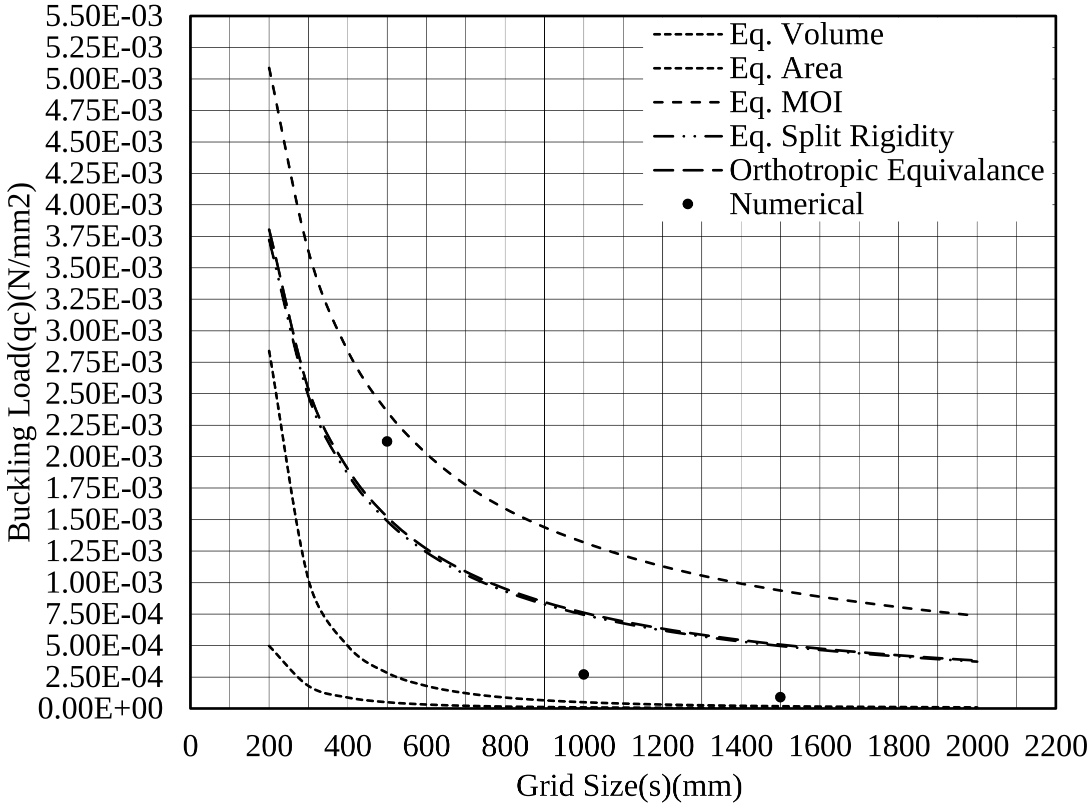

Figure 5.14: Comparison of buckling load (Quadrilateral grid, r=20)

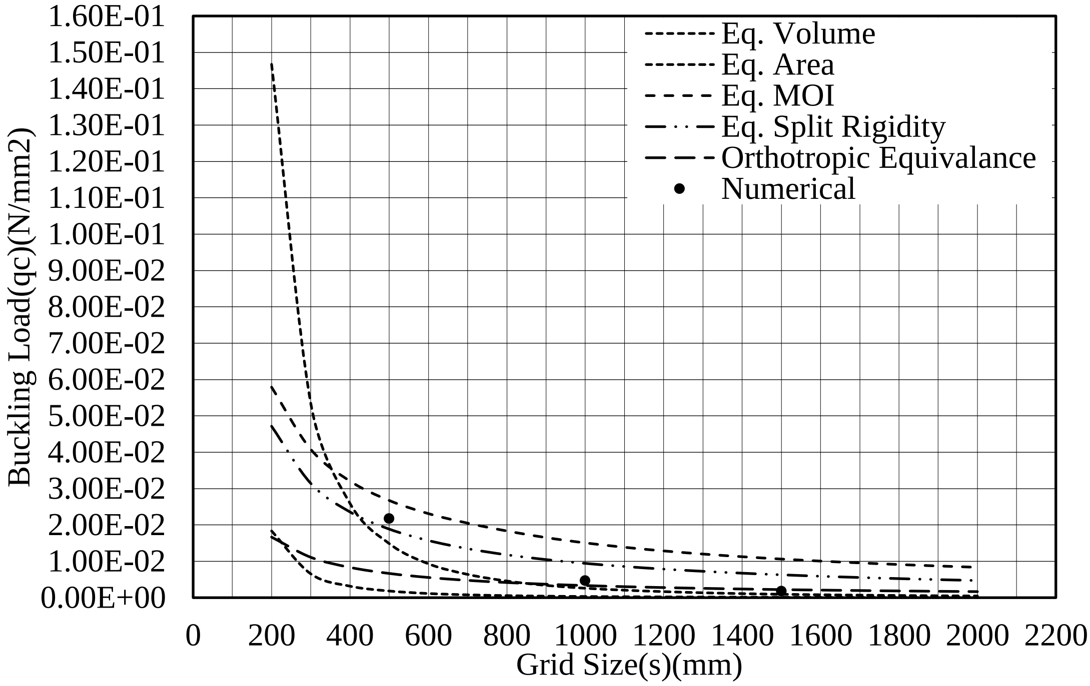

Figure 5.15: Comparison of buckling load (Triangular grid, r=5)

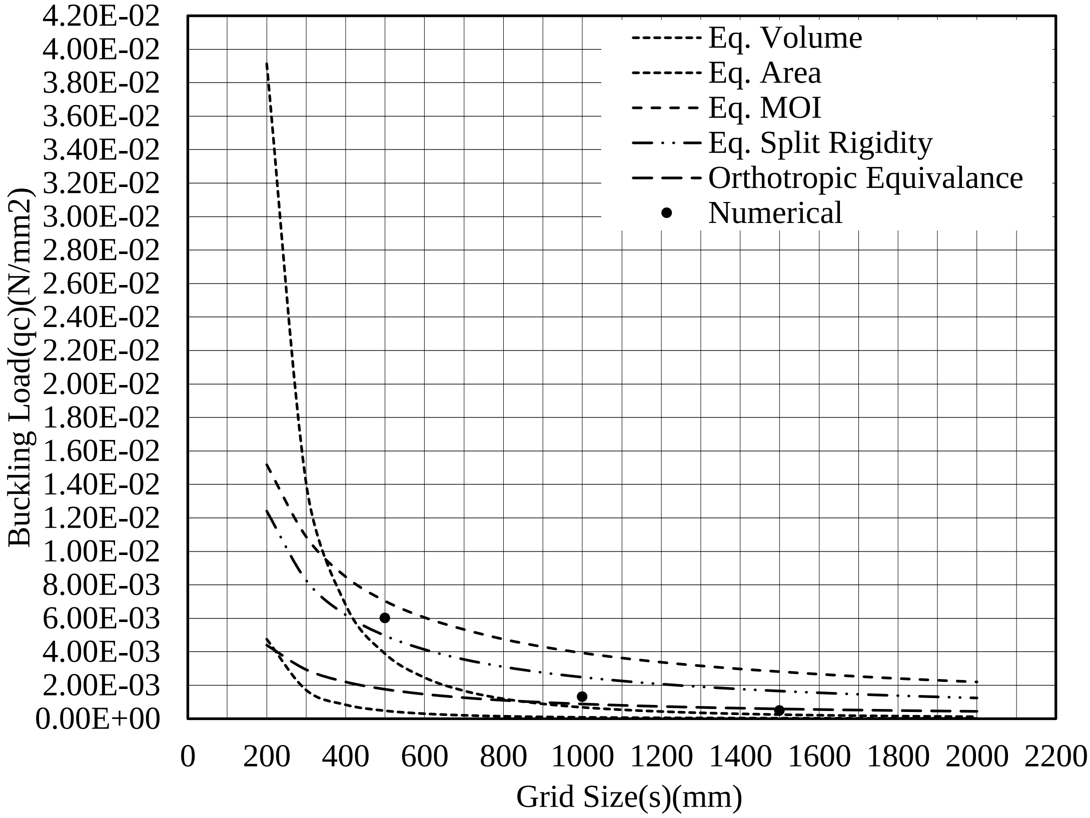

Figure 5.16: Comparison of buckling load (Triangular grid, r=14)

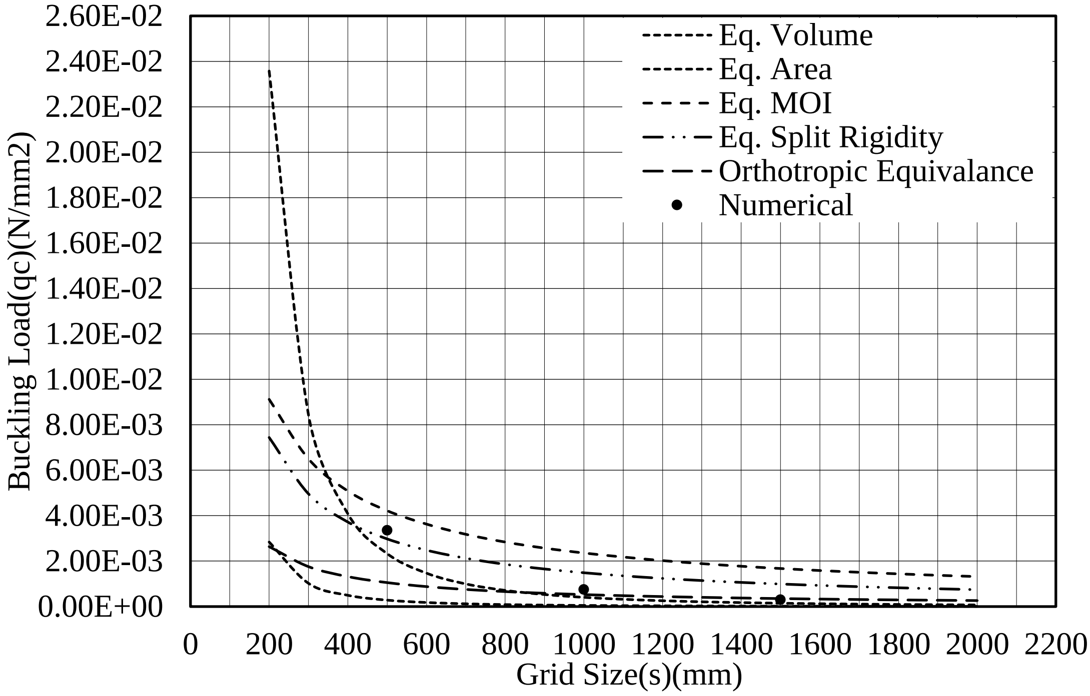

Figure 5.17: Comparison of buckling load (Triangular grid, r=20)

As explained in Chapter 4.2, the analytical solution for the equivalent area model and equivalent moment of inertia model always gives the lower and upper bound solution respectively. All the numerical results fall well between the lower and upper bound. From the graphical plots, it is clear that the denser grid shows more bending dominated characteristics whereas the coarser grid shows more membrane dominated characteristics. A factor β_q is defined in Eq. 5.1 which gives the degree of membrane characteristics. Value of $\beta_q > 1$ indicates that the behaviour of grid shell is membrane dominated.

$$\beta_q = \frac{(q_c)_{Eq.\ MOI} - (q_c)_{Numerical}}{(q_c)_{Numerical} - (q_c)_{Eq.\ Area}} \tag{Eq. 5.1}$$

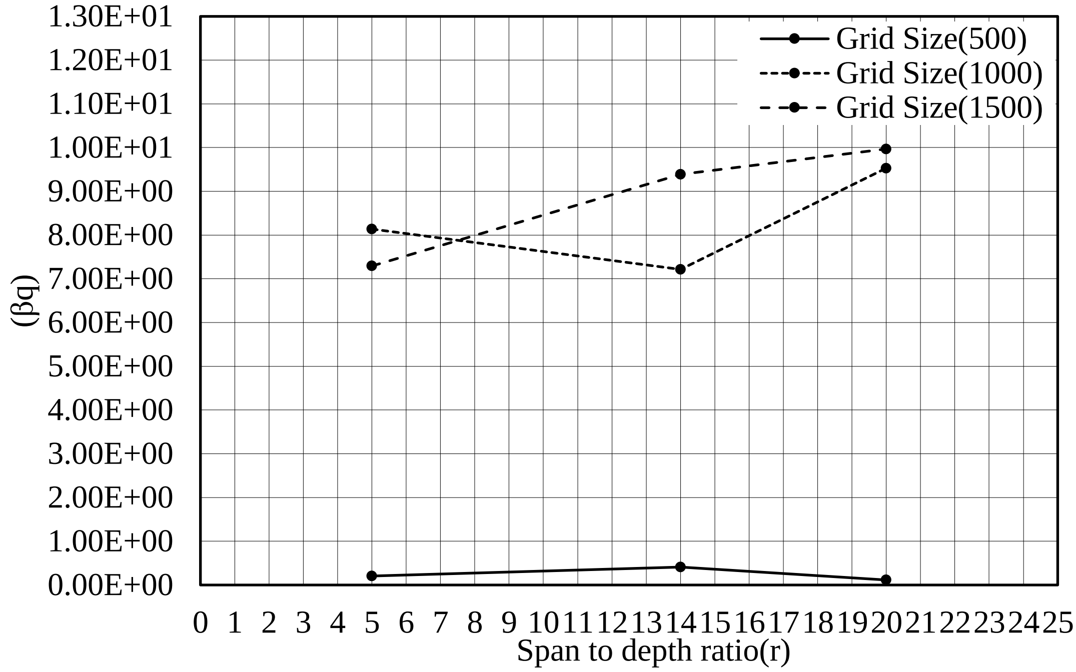

Figure 5.18: Degree of membrane dominance for the quadrilateral grid (β_q)

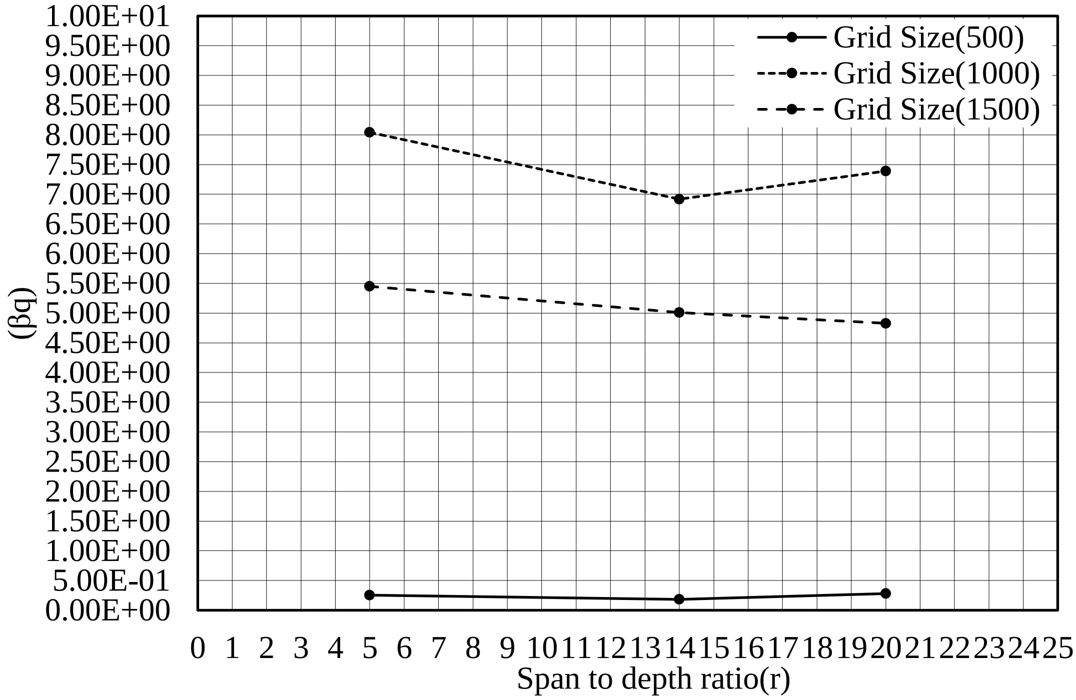

Figure 5.19: Degree of membrane dominance for the triangular grid (β_q)

Figure 5.18 and Figure 5.19 shows the variation of β_q with grid size and span to depth ratio. The value of β_q for grid size 1000mm and 1500mm remains well above 1. For grid size 500mm value of β_q remains well below 1. So, it can be concluded that for the denser grid (500mm) grid shell remains bending dominated with the increase in shallowness but for the coarser grid (>1000mm) grid shell remains membrane dominated with the increase in shallowness. An equivalent model cannot estimate the buckling load of the grid shell with considerable accuracy. But the equivalent model can yield a conservative value at the beginning of the design process which can omit the risk of changing the parameters after structural design. For coarser grid size (>1000mm) equivalent volume model is the best model to calculate the buckling load of the grid shell. For denser grid size (500mm), the orthotopic equivalence model for the quadrilateral grid and equivalent split rigidity model for the triangular grid can yield a conservative value of buckling load.

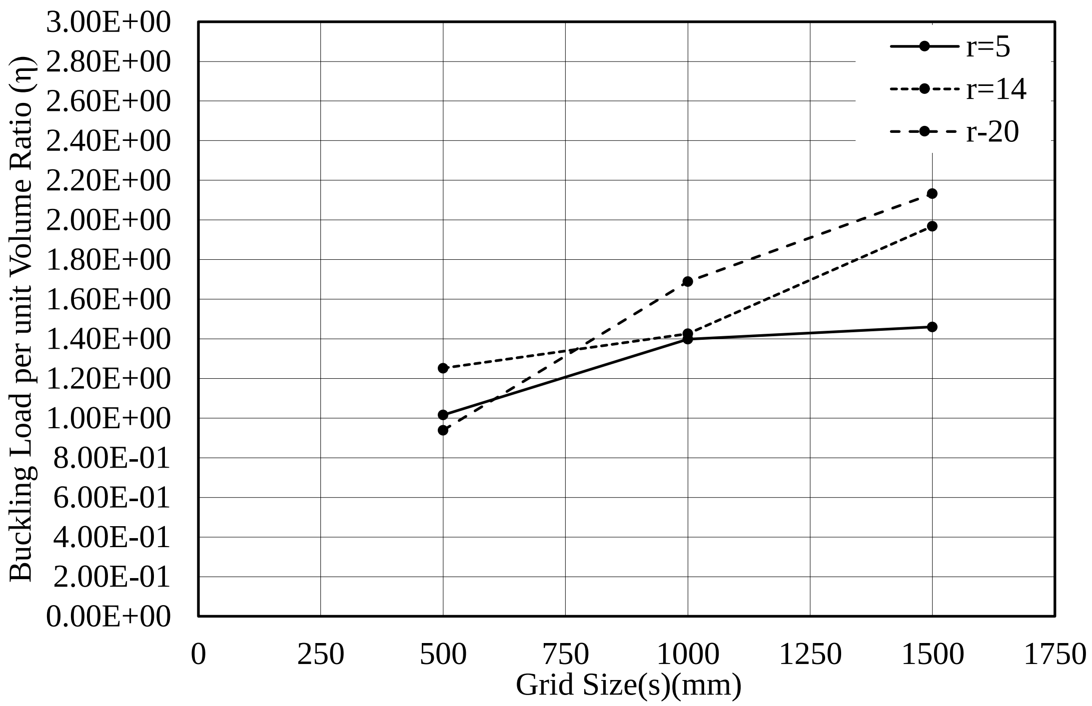

Figure 5.20: Efficiency of grid shell

Figure 5.20 shows the efficiency of the grid shell. The ratio η is defined as $\eta = \frac{(q_c)_{triangular}\ per\ unit\ volime}{(q_c)_{quadrilateral}\ per\ unit\ volume}$. The load carrying capacity for the triangular grid is higher as it has a higher in-plane stiffness. But the use of a triangular grid increases the no. of the grid element. The ratio η incorporates both load carrying capacity and no. of grid element. The triangular grid is more efficient for coarser grid size.

5.6 Discussion

In this thesis, an open circular-cylindrical shell of span(L) 15000mm, length(l) 30000mm and span to depth ratio(r) 5, 14 & 20 are considered for analysis. In the design and construction of the grid shell, its geometrical properties are described in terms of span and span to depth ratio. But in analytical solution span and radius of curvature describes the geometrical properties. For span to depth ratios 5, 14 & 20 the radius of curvature (the radius for cylindrical shell) are 10875mm, 26785,71mm & 37875mm respectively. The results can also be analyzed in terms of the radius of curvature. Ratio L/a describes the type of shell as short, intermediate and long. The range of L/a with equivalent thickness from equivalent models indicates the grid shell considered is intermediate. For the intermediate shell, the value of buckling load is different for different parameters but the pattern of values remains the same for the equivalent models. As the numerical results fall well within the bound, the conclusions drawn from the result of this thesis can be applied for the intermediate grid shell.

The failure mode of a single-layered gird shell is buckling. So, the higher value of buckling load higher is the load-carrying capacity of the grid shell. Grid sizes considered here are 500mm, 1000mm and 1500mm. A grid size of about 500mm is considered a denser grid whereas a grid size $\geq$ 1000mm is considered a coarser grid. As the grid size increases load-carrying capacity of the grid shell decreases. For a steeper shell a coarser grid can also result in a significantly high load carrying capacity but for a shallower shell coarser grid results in a very low load-carrying capacity. A coarse grid can be used for a steeper grid shell but the use of a dense grid is suggested for a shallower grid shell.

The numerical value of buckling load of grid shell falls well within the bound of membrane and bending characteristics. A denser grid shows bending dominated characteristics whereas a coarser grid shows membrane dominated characteristics. With the increase in span to depth ratio bending characteristics remains the same for the denser grid, but the coarser grid membrane characteristics remain the same. The load-carrying capacity of grid shells decreases with increases in span to depth ratio.

The triangular grid shows more load-carrying capacity than the quadrilateral grid as it has more in-plane stiffness. The triangular grid shows 2 to 3 times more capacity than the quadrilateral grid. The ratio η defines the efficiency of grid type, the triangular grid is more efficient for coarser grid size.

Different equivalent models act as a tool for calculating the load-carrying capacity of grid shells analytically. Equivalent area and equivalent moment of inertia give the lower and upper bound for it. For coarser grid equivalent volume model and, denser grid orthotropic equivalence model for the quadrilateral grid and equivalent split rigidity model for the triangular grid can be used to calculate the load-carrying capacity of grid shell.

CHAPTER 6: CONCLUSIONS

6.1 Summary and Conclusions

The objectives described in Chapter 1.5 are achieved by conducting a parametric analysis of an open circular-cylindrical grid shell varying grid size, grid type and span to depth ratio and calculating the load-carrying capacity of grid shells using both analytical and numerical methods. Different continuum models are used to define grid shells as equivalent continuous shells. The equation for calculating the buckling load of the continuous shell is modified to accommodate the equivalent properties of the grid shell and an analytical solution is achieved. Geometries are modelled in ANSYS and the numerical solution is achieved. Comparison of analytical and numerical results is presented in graphical plot form. The conclusions are summarized in the following points:

1. For coarser grid equivalent volume model and, denser grid orthotropic equivalence model for the quadrilateral grid and equivalent split rigidity model for the triangular grid is suggested as an approximate equivalent model.
2. The load-carrying capacity for the triangular grid is 2 to 3 times more than the quadrilateral grid. The triangular grid is more efficient for coarser grid size. Also, the triangular grid is more efficient for shallower shells.
3. Denser grid shows bending dominated characteristics whereas the coarser grid shows membrane dominated characteristics. The bending or membrane dominance characteristics are defined based on the closeness of numerical value of buckling load with the equivalent moment of inertia model (Upper bound) and equivalent area model (Lower bound) respectively.
4. For denser grid bending dominated characteristics remains the same with an increase in shallowness whereas for coarser grid membrane dominated characteristics remains the same with an increase in shallowness.

6.2 Recommendations for Further Work

Parametric stability analysis of open circular-cylindrical grid shells has been conducted. But the analysis has been performed with some limitations. This motivates other areas for continued research.

1. The shape considered here is an open circular-cylindrical grid shell. Other shapes of grid shells can also be analyzed.

2. The connection considered is rigid. The effect of flexibility of connection on the load-carrying capacity of grid shells may be studied.
3. Non-linear and post-buckling behaviour of grid shells may be studied.
4. The effect of unsymmetrical loading may be analyzed.
5. Local instability and snap-through buckling behaviour may be studied.

REFERENCES

Bulenda, T. & Knippers, J., 2001. Stability of grid shells. *Computers & Structures,* 79(12), pp. 1161-1174.

Douthe, C., Baravel, O. & Caron, J., 2006. Form-finding of a grid shell in composite materials. *Journal of the International Association for Shell and Spatial Structures,* 47(1), pp. 53-62.

Farshad, M., 1992. *Design and Analysis of Shell Structures.* 1st ed. Dordrecht: Springer Science & Business Media.

Forman, S. E. & Hutchinson, J. W., 1970. Buckling of Reticulated Shell Structures. *International Journal of Solids Structures*, 6(7), pp. 909-932.

Gioncu, V., 1985. Instability Problems in Space Structures. *International Journal of Space Structures*, 1(3), pp. 169-183.

Gioncu, V., 1995. Buckling of Reticulated Shells. state-of-the-art. *International Journal of Space Structures,* 10(1), pp. 1-46.

Gioncu, V. & Balut, N., 1992. Instability behaviour of single layer reticulated shells. *International journal of space structures,* 7(4), pp. 243-252.

Green, H. & Lauri, D., 2017. Form Finding of Grid Shells a Parametric Approach using Dynamic Relaxation, M.Sc. Thesis. *Royal Institute of Technology*.

Kato, S., Yamauchi, Y. & Ueki, T., 2005. Buckling Load of Elliptic Paraboloidal Single Layer Reticulated Roofs Under Uniform Load. *International Journal of Space Structures,* 20(2), pp. 91-106.

Malek, R. S., 2012. The Effect of Geometry and Topology on The Mechanics of Grid Shells, Ph.d. Thesis. *Massachusetts Institute of Technology.*

Mesnil, R., 2013. Stability of Elastic Grid Shells, M.E. Thesis. *Massachusetts Institute of Technology.*

Mesnil, R., Douthe, C., Baverel, O. & Leger, B., 2017. Linear buckling of quadrangular and kagome gridshells: a comparative assessment. *Engineering Structures,* Volume 132, pp. 337-348.

Noor, A. K., 1988. Continuum Modeling for Repetitive Lattice Structures. *Applied Mechanics Reviews,* 41(7), pp. 285-296.

Pshenichnov, G. I., 1993. *A Theory of Latticed Plates and Shells.* s.l.:World Scientific Publishing Co. Pte. Ltd..

Schober, H., 2015. *Transparent Shells, Form, Topology, Structure.* Stuttgart: Ernst & Sohn, A Wiley Brand.

Showkati, H. & Ansourian, P., 1996. Influence of Primary Boundary Conditions on the Buckling of Shallow Cylindrical Shells. *Journal of Constructional Steel Research,* 36(1), pp. 53-75.

Sumec, J., 1992. General stability analysis of lattice shells by continuum modeling. *International Journal of Space Structures*, 7(4), pp. 275-283.

Timoshenko, S. P. & Gere, J. M., 1985. *Theory of Elastic Stability.* 2nd ed. s.l.:McGraw-Hill International Book Company.

Timoshenko, S. & Woinowsky-Krieger, S., 1959. *Theory of Plates and Shells.* 1st ed. New York: McGraw-Hill Book Company.

Ventsel, E. & Krauthammer, T., 2001. *Thin Plates and Shells Theory, Analysis, and Applications.* New York: Marcel Dekker, Inc..

Zienkiewicz, O. C. & Taylor, R. L., 2005. *The finite element method for solid and structural mechanics.* 6th ed. s.l.:Elsevier.

ANNEX A: FLOWCHART AND SOURCE CODE

A.1 Flow Chart

A program in MATLAB is written to achieve an analytical solution of the buckling load of the grid shell. Flowchart for the source code in MATLAB is presented in Figure A.1.

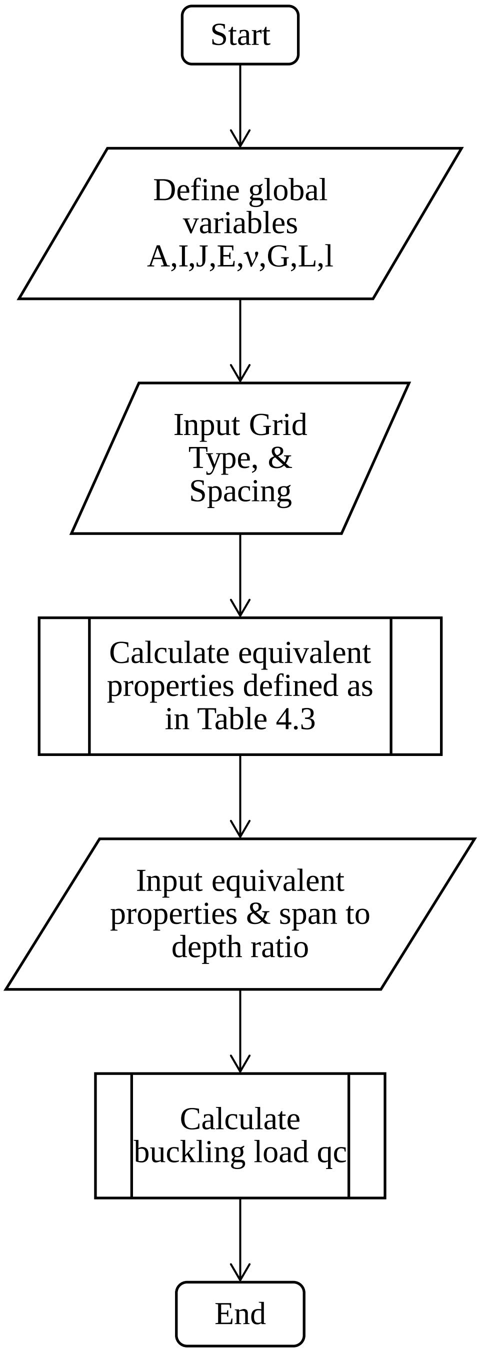

Figure A.1: Flowchart for source code in MATLAB

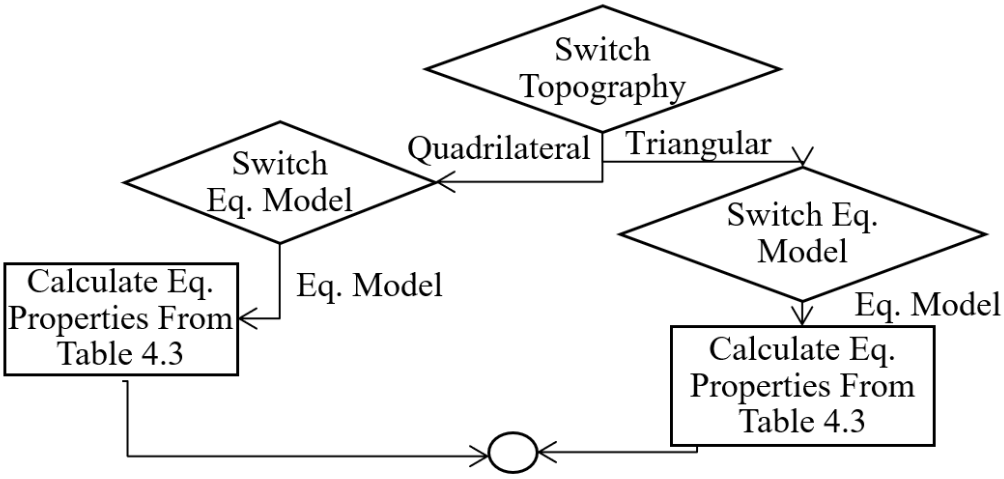

Figure A.2: Flowchart for sub-function for calculating equivalent properties

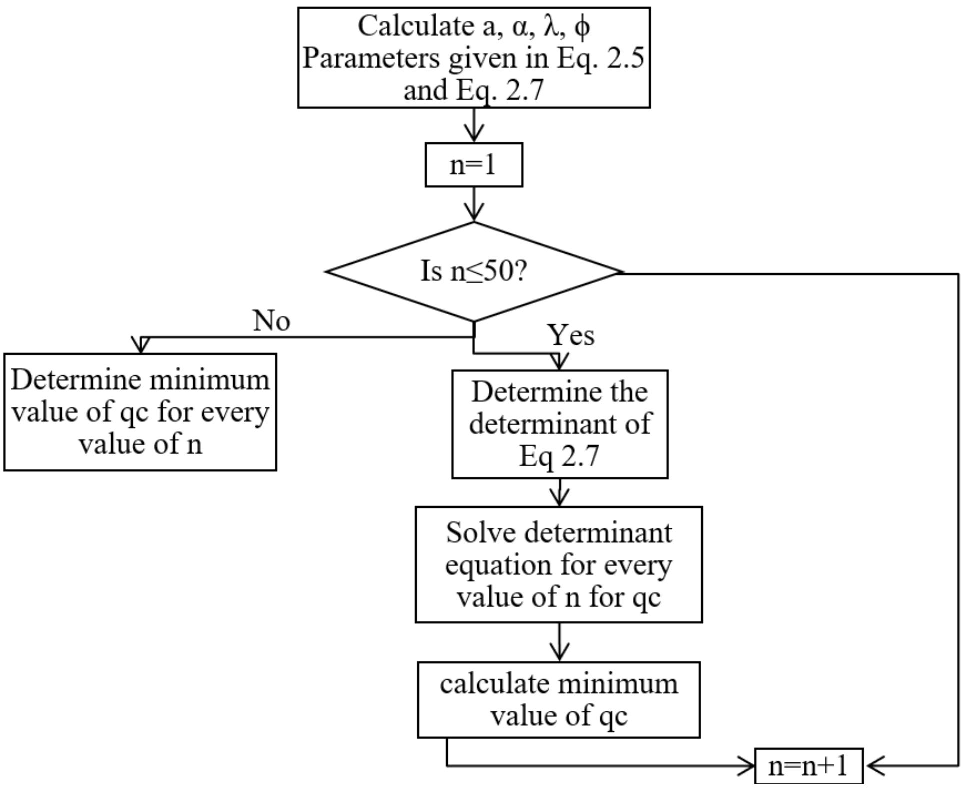

Figure A.3: Flowchart for sub-function for calculating buckling load

A.2 Source code in MATLAB

In MATLAB the built-in functions for calculating determinants, solving quadratic equations, etc. are utilized. Looping functions are used for iterative processes.

```
**************************************************************
% Buckling of Grid Shell
% Units are in N and mm
% Definition of Global Variable

global A I J E nu G L l
```

```
% Properties of grid element(rod)

A=50*                                    % Area of
Rod(mm2)
I=50^4/12;                          % Moment of
Inertia(mm4)
J=0.141*50^4;             % Torsional Moment of
Inertia(mm4)
E=210000;                      % Modulus of
Elasticity(N/mm2)
nu=0.3;  m                               % Poission`s
Ratio
G=E/(2*(1+nu));                  % Modulus of
Rigidity(N/mm2)
L=15000;                              % Span of Grid
Shell(mm)
l=30000;                            % Length of Grid
Shell(mm)

% r=Span to Depth Ratio
% r=5,14,20
% s=Grid Size (Spacing)
% heq=Equivalent Thickness
% Ceq=Equivalent Axial Rigidity
% Deq=Equivalent Bending Rigidity
% nuc=Poission`s Ratio for Axial Rigidity
% nud=Poission`s Ratio for Bending Rigidity
% Topology='tria','quad'
% 'tria'=Triangular
% 'quad'=Quadrilateral
% Model='eqvol','eqarea','eqmoi','eqsprig','eqortho'
% 'eqvol'=Equivalent Volume
% 'eqarea'=Equivalent Area
% 'eqmoi'=Equivalent Moment of Inertia
% 'eqsprig'=Equivalent Split Rigidity
% 'eqortho'= Orthotropic Equivalence
% qc=Buckling Load
model={'eqvol','eqarea','eqmoi','eqsprig','eqortho'};
qc=zeros();
for j=1:1:5
    for i=1:1:19
    s=(i+1)*100;
[Ceq,Deq,nuc,nud]=Equivalent_Properties('tria',char(model
(j)),s);
    qc(i,j)=Buckling_Continuous(Ceq,Deq,nuc,nud,20);
    end
end
*********************************************************
function
[Ceq,Deq,nuc,nud]=Equivalent_Properties(topography,model,
s)
```

```
% Calculation of Equivalent Properties

global A I J E nu G
switch(topography)              % Triangular/Quadrilateral
    case 'quad'                            % Quadrilateral
        switch(model)
            case 'eqvol'                 % Equivalent Volume
                heq=2*A/s;
                [Ceq,Deq]=Equivalent_Rigidity(heq);
                nuc=nu;
                nud=nu;
            case 'eqarea'                  % Equivalent Area
                heq=A/s;
                [Ceq,Deq]=Equivalent_Rigidity(heq);
                nuc=nu;
                nud=nu;
            case 'eqmoi'    % Equivalent Moment of Inertia
                heq=(12*I/s)^(1/3);
                [Ceq,Deq]=Equivalent_Rigidity(heq);
                nuc=nu;
                nud=nu;
            case 'eqsprig'     % Equivalent Split Rigidity
                Ceq=E*A/s;
                Deq=E*I/s;
                nuc=nu;
                nud=nu;
            case 'eqortho'       % Orthotropic Equivalence
                Ceq=E*A/s;
                Deq=E*I/s;
                nuc=0;
                nud=0;
        end
    case 'tria'
        switch(model)
            case 'eqvol'
                heq=8*A/(sqrt(3)*s);
                [Ceq,Deq]=Equivalent_Rigidity(heq);
                nuc=nu;
                nud=nu;
            case 'eqarea'
                heq=2*A/s;
                [Ceq,Deq]=Equivalent_Rigidity(heq);
                nuc=nu;
                nud=nu;
            case 'eqmoi'
                heq=(24*I/s)^(1/3);
                [Ceq,Deq]=Equivalent_Rigidity(heq);
                nuc=nu;
                nud=nu;
            case 'eqsprig'
```

```
                Ceq=2*E*A/s;
                Deq=2*E*I/s;
                nuc=nu;
                nud=nu;
            case 'eqortho'
                Ceq=9*E*A/(8*s);
                gam=G*J/(E*I);
                Deq=3*E*I*(1+gam)/(8*s);
                nuc=1/3;
                nud=(1-gam)/(3+gam);
        end
end
end
*********************************************************
function [ceq,deq] = Equivalent_Rigidity(heq)
global E nu
ceq=E*heq/(1-nu^2);
deq=E*heq^3/(12*(1-nu^2));
end
*********************************************************
function [qc]= Buckling_Continuous(Ceq,Deq,nuc,nud,r)

% Calculation of Buckling Load of Equivalent Continuous
Shell

% qc=Load
% n=Buckling Mode

global L l
syms q eival
a=L/2*(r/4+1/r);
phi=q*a/Ceq;                                  % Phi Parameter
alph=Deq/(Ceq*a^2);                          % Alpha Parameter
lam=a*pi()/l;                                % Lamda Parameter

% Solution of Eigen Value Problem

qn=zeros();
for n=2:1:50
eival(1,1)=-(lam^2+(1-nuc)/2*n^2);
eival(1,2)=n*lam*((1+nuc)/2+phi);
eival(1,3)=lam*(nuc+phi);
eival(2,1)=(1+nuc)/2*n*lam;
eival(2,2)=-((1-nuc)/2*lam^2+n^2+alph*n^2+alph*(1-
nud)*lam^2);
eival(2,3)=-(n+alph*n*lam^2+alph*n^3);
eival(3,1)=nuc*lam;
eival(3,2)=-(n+alph*n^3+alph*(2-nud)*n*lam^2);
eival(3,3)=-
(1+alph*lam^4+alph*n^4+2*alph*lam^2*n^2+phi*(1-n^2));
y=det(eival)==0;
```

```
sol=solve(y,q);
qn(n-1)=min(double(sol));
end
qc=min(qn);
end
```

```
**********************************************************
```

A.3 Visual Code in Grasshopper

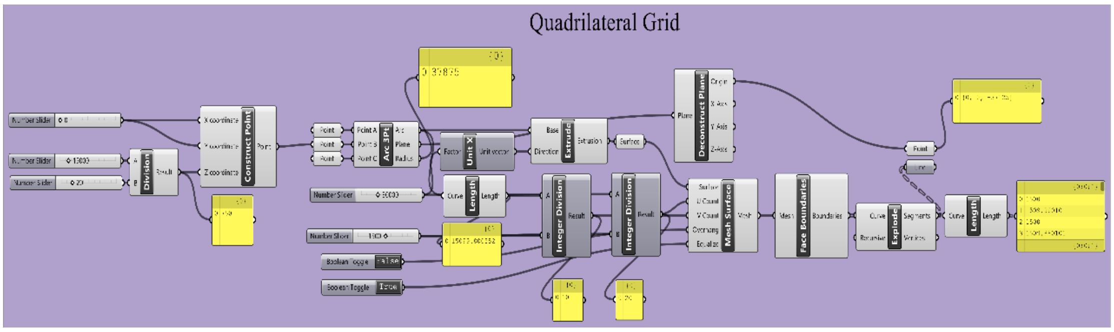

Figure A.4: Visual code in Grasshopper for quadrilateral grid

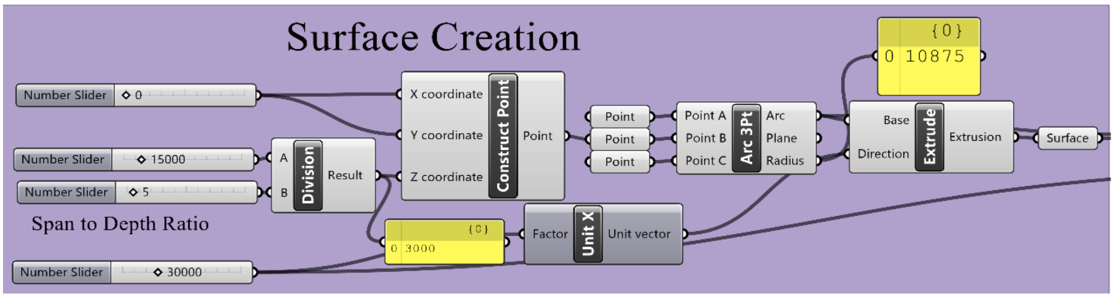

Figure A.5: Visual code in Grasshopper for surface creation for a triangular grid

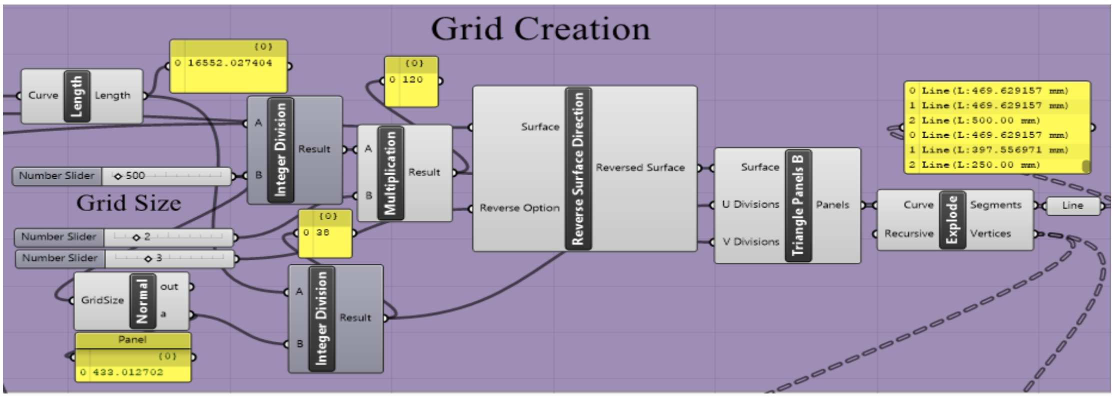

Figure A.6: Visual code in Grasshopper for grid creation for a triangular grid